ORIGINAL RESEARCH

# Nucleotide-Binding Oligomerization Domain-Like Receptor Protein 3 Deficiency in Vascular Smooth Muscle Cells Prevents Arteriovenous Fistula Failure Despite Chronic Kidney Disease

Xiangchao Ding, MD;* Jiuling Chen, MD;* Chuangyan Wu, MD;* Guohua Wang, MD; Cheng Zhou, MD; Shanshan Chen, MD; Ke Wang, MD; Anchen Zhang, MD; Ping Ye, MD; Jie Wu, MD; Shanshan Chen, MD; Hao Zhang, MD; Kaiying Xu, MD; Sihua Wang, MD; Jiahong Xia, MD, PhD

***Background*—**The arteriovenous fistula (AVF) is the preferred hemodialysis access for patients with chronic kidney disease. Chronic kidney disease can increase neointima formation, which greatly contributes to AVF failure by an unknown mechanism. Our study aimed to determine the role of nucleotide-binding oligomerization domain-like receptor protein 3 (NLRP3) in neointima formation induced by experimental AVFs in the presence of chronic kidney disease.

***Methods and Results*—**From our findings, NLRP3 was upregulated in the intimal lesions of AVFs in both uremic mice and patients. Smooth muscle–specific knockout NLRP3 mice exhibited markedly decreased neointima formation in the outflow vein of AVFs. Compared with primary vascular smooth muscle cells isolated from control mice, those isolated from smooth muscle–specific knockout NLRP3 mice showed compromised proliferation, migration, phenotypic switching, and a weakened ability to activate mononuclear macrophages. To identify how NLRP3 functions, several small-molecule inhibitors were used. The results showed that NLRP3 regulates smooth muscle cell proliferation and migration through Smad2/3 phosphorylation rather than through caspase-1/interleukin-1 signaling. Unexpectedly, the selective NLRP3-inflammasome inhibitor MCC950 also repressed Smad2/3 phosphorylation and relieved chronic kidney disease–promoted AVF failure independent of macrophages.

***Conclusions*—**Our findings suggest that NLRP3 in vascular smooth muscle cells may play a crucial role in uremia-associated AVF failure and may be a promising therapeutic target for the treatment of AVF failure. **(*J Am Heart Assoc*. 2019;8:e011211. DOI: 10.1161/JAHA.118.011211)**

**Key Words:** arteriovenous fistula • chronic kidney disease • NLRP3 • SMAD

The arteriovenous fistula (AVF) is a preferred vascular access for patients with end-stage renal disease, but its patency rate is only 60% in the first year, with 35% failure after 2 years.[1,2] The main cause of AVF failure is intimal hyperplasia (IH), and another major weakness of AVFs is the time it takes for the fistula to mature.[3] Adequate outward remodeling could preserve luminal caliber and may, therefore, be valuable for successful fistula maturation.[4] Recent studies showed that chronic kidney disease (CKD)–promoted cytokine secretion and vascular smooth muscle cell (VSMC) migration and proliferation are associated with IH formation,[1,2] suggesting that CKD plays a notable role in AVF failure, with systemic

*From the Departments of Cardiovascular Surgery (X.D., J.C., C.W., G.W., C.Z., J.W., S.C., H.Z., J.X.) and Thoracic Surgery (C.W., K.X., S.W.), Union Hospital, and Key Laboratory for Molecular Diagnosis of Hubei Province (S.C.), Central Laboratory (S.C.) and Department of Cardiovascular Medicine (A.Z., P.Y.), Central Hospital of Wuhan, and Department of Respiratory and Critical Care Medicine, Tongji Hospital (K.W.), Tongji Medical College, Huazhong University of Science and Technology, Wuhan, China.*

Accompanying Tables S1, S2 and Figures S1 through S8 are available at https://www.ahajournals.org/doi/suppl/10.1161/JAHA.118.011211

*Dr Xiangchao Ding, Dr Jiuling Chen, and Dr Chuangyan Wu contributed equally to this work.

**Correspondence to:** Jiahong Xia, MD, PhD, Department of Cardiovascular Surgery, Union Hospital, Tongji Medical College, Huazhong University of Science and Technology, No. 1277, Jiefang Rd, Wuhan 430022, China. E-mail: jiahong.xia@hust.edu.cn; Sihua Wang, MD, Department of Thoracic Surgery, Union Hospital, Tongji Medical College, Huazhong University of Science and Technology, No. 1277, Jiefang Rd, Wuhan 430022, China. E-mail: sihua_wang@126.com

Received October 13, 2018; accepted November 27, 2018.

## Clinical Perspective

### What Is New?

- Nucleotide-binding oligomerization domain-like receptor protein 3 (NLRP3) was upregulated in the intimal lesions of arteriovenous fistulas (AVFs), and smooth muscle–specific knockout NLRP3 attenuates AVF neointima formation.
- NLRP3 knockout inhibits smooth muscle cells phenotypic transformation via Smad2/3 suppression.
- MCC950 administration resulted in tolerance to AVF-induced neointima formation despite chronic kidney disease.

### What Are the Clinical Implications?

- Our findings suggest that NLRP3 in vascular smooth muscle cells play a crucial role in uremia-associated AVF failure; thus, specifically targeting VSMCs and NLRP3 may be a promising approach for treating AVF failure.

effects.[3,5,6] A healthy vein has the potential for successful outward remodeling; however, adequate maturation may be partially hindered by CKD-induced vasculopathy, such as IH.[4]

IH is characterized by an abundance of smooth muscle cells (SMCs), myofibroblasts, fibroblasts, and macrophages that induce venous outflow obstruction, which is a leading cause of stenosis and blood flow reduction or thrombosis.[3,7] Several vascular biology pathways are involved in IH pathology, including inflammation, uremia, hypoxia, shear stress, and thrombosis. These mechanisms are thought to work in concert through linked cytokine cascades and, possibly, epigenetic changes, resulting in negative remodeling and fistula failure.[3,8]

The nucleotide-binding oligomerization domain-like receptor protein 3 (NLRP3) inflammasome is a cytosolic complex that participates in early inflammatory responses. On activation, NLRP3 forms a complex with its adaptor apoptosis-associated speck-like protein containing a caspase-recruitment domain (ASC), which facilitates the conversion of procaspase-1 to active caspase-1.[9] The activated caspase-1 processes pro-interleukin-1β into its mature form, interleukin (IL)-1β, and triggers a related inflammatory response.[10] NLRP3 inflammasome signaling is involved in various disease pathogeneses, such as atherosclerosis,[11] myocardial infarction,[12] and insulin resistance.[13]

The latest reports indicated that NLRP3 might be crucial to VSMCs and showed that NLRP3 was involved in VSMCs phenotypic switching in hypertension.[14] Moreover, NLRP3 promotes contractile protein degradation in SMCs, which contribute to accelerate abdominal aortic aneurysm or thoracic aortic aneurysm formation.[15,16] In addition to the inflammasome signaling pathway, NLRP3 and ASC in fibroblasts[17] or dendritic cells[18] seem to be required for Smad2/3 phosphorylation, which is a critical pathway in VSMCs.[19,20] Yet, the role of NLRP3 in the physiological process of CKD-induced changes in VSMCs and neointima formation in AVFs is poorly defined. Therefore, this study aimed to determine the role of NLRP3 in IH induced by experimental AVFs in the presence of CKD.

## Materials and Methods

The data, analytic methods, and study materials will not be made available to other researchers for purposes of reproducing the results or replicating the procedure. Other researchers may contact the corresponding author about the data and methodological questions.

### Human Samples

Great saphenous vein samples without varicosity (used as a control) were obtained from patients undergoing coronary bypass surgery. Outflow vein samples with neointimal hyperplasia were obtained from patients who agreed to undergo surgical AVF revision because of a low AVF flow, as previously described.[21] These samples were collected for pathological examination or for total protein extraction. Background characteristics of patients are shown in Table S1.

The study was conducted according to the Declaration of Helsinki and approved by the Union Hospital Medical Ethics Committee of Huazhong University of Science and Technology. Written informed consent was obtained from patients or family members.

### Mice

All animal experiments were performed in a specific pathogen-free barrier facility in accordance with the institutional guidelines and an approved protocol (IORG o: IORG0003571) of Tongji Medical College, Huazhong University of Science and Technology. All animals were male and kept in a 12-hour light/dark cycle. *NLRP3*$^{fl/fl}$ mice (with a C57BL/6 background) were generated by the Model Animal Research Center of Nanjing University (Nanjing, China). *Smooth muscle protein 22 alpha* (*SM22α*)-*CreER*$^{T2}$ mice were purchased from Shanghai Model Organisms Center, Inc (Shanghai, China). C57BL/6 mice were purchased from HFK Bioscience (Beijing, China). Smooth-muscle-specific knockout NLRP3 (*NLRP3*$^{SMC\ KO}$) mice were generated by crossing *NLRP3*$^{fl/fl}$ with *SM22α-CreER*$^{T2}$ mice, and *NLRP3*$^{fl/fl}$ mice that were not introduced to Cre recombinase were used as littermate controls. Tamoxifen (Sigma, Shanghai, China) was dissolved in corn oil (20 mg/mL) and administered by oral

gavage at the indicated time (0.1–0.15 mg tamoxifen/g mouse body weight) in both *NLRP3*$^{SMC\ KO}$ mice and *NLRP3*$^{fl/fl}$ littermates.

## Murine Models of CKD and AVF

CKD was induced by subtotal nephrectomy in anesthetized mice as described.[22,23] Briefly, approximately two thirds of the left kidney was resected. Postoperatively, mice received a 6% protein diet to reduce mortality, and then the right kidney was removed 1 week later. Mice received a 40% protein diet 1 week after right kidney removal. The serum of mice was collected 3 weeks after right kidney removal, and blood urea nitrogen and creatinine levels were measured by an automated chemistry analyzer (Chemray 420; Rayto, Shenzhen, China). AVF was created by an end-vein to side-artery anastomosis of the left external jugular vein and the left common carotid artery 3 weeks after right nephrectomy.[23] AVFs were collected to assess for morphological changes. The mice received intraperitoneally MCC950 (10 mg/kg body weight) or a vehicle (0.9% NaCl) every other day after AVF surgery. Blood urea nitrogen, serum creatinine, body weight, blood pressure, and heart rate of *NLRP3*$^{SMC\ KO}$ mice, *NLRP3*$^{fl/fl}$ littermates, or MCC950/vehicle-treated wild-type (WT) mice with CKD were measured on postoperative days (POD) 21. For macrophage depletion, the mice were injected with ≈50 mg/kg of clodronate liposomes intraperitoneally or an equal volume of PBS liposomes. The injection was repeated 3 days later, and AVFs were performed 6 to 7 days after the first injection; macrophage clearance by clodronate liposomes was verified using flow cytometry.

## Quantitative Real-Time Polymerase Chain Reaction

Total RNA was obtained using the TRIzol reagent (Invitrogen, Carlsband, CA). A complementary DNA synthesis kit (Takara, Dalian, China) was applied for complementary DNA synthesis. Quantitative real-time polymerase chain reaction (qPCR) was performed using SYBR Premix Ex Taq (Takara) following the manufacturer's protocol on an ABI StepOne Plus System (Applied Biosystems, Framingham, MA). Messenger RNA (mRNA) expressions were normalized using GAPDH as an internal control and analyzed by $2^{-\Delta\Delta Ct}$. The primers listed in Table S2 were designed by Sangon Biotech (Shanghai, China). All the qPCR results were performed in triplicate.

## Western Blot

Harvested tissues and cells were lysed on ice using RIPA Lysis Buffer (Beyotime, Shanghai, China) containing a protease inhibitor PMSF (Beyotime). Western blot was performed as previously described.[24] Anti-NLRP3 (Abcam ab214185, 1:1000 dilution), anti-ASC (Santa Cruz Biotechnology sc-514414, 1:1000 dilution), anti-caspase-1 (Abcam ab179515, 1:1000 dilution), anti-IL-1β (Cell Signaling Technology 12242, 1:1000 dilution), anti-α-smooth muscle actin (α-SMA, Sigma-Aldrich A2547, 1:1000 dilution), anti-SM22α (Abcam ab14106, 1:1000 dilution), anti-osteopontin (OPN, Abcam ab8448, 1:1000 dilution), anti-P-Smad2/3 (Cell Signaling Technology 8828, 1:1000 dilution), anti-Smad2/3 (Cell Signaling Technology 8685, 1:1000 dilution), and anti-GAPDH (Cell Signaling Technology 8884, 1:1000 dilution) were used as primary antibodies. HRP-labeled goat anti-rabbit immunoglobulin (Ig)-G or goat anti-mice IgG were used as secondary antibodies. The protein signals were visualized and analyzed using the ChemiDocTM XRS+ system (Bio-Rad, Hercules, CA). The intensity of the Western blot band was determined using ImageJ software (http://rsb.info.nih.gov/ij/). Images of the original uncropped blots of a representative Western blot are provided in Figure S1.

## Histology

We harvested the great saphenous vein, failed AVFs, and outflow vein, including the anastomosis, at various time points. After formaldehyde fixation, dehydration, and paraffin embedding, 5-μm serial sections were obtained for hematoxylin and eosin staining and immunohistochemistry. Procedures were performed as described previously.[21] Primary antibodies included anti-NLRP3 (Abcam ab4207, 1:100 dilution), anti-CD68 (Abcam ab955, 1:100 dilution), anti-Ki67 (Abcam ab15580, 1:100 dilution), anti-calponin 1 (CNN1, Abcam ab46794, 1:100 dilution), anti-proliferating cell nuclear antigen (PCNA, Abcam ab29, 1:100 dilution), and anti-α-SMA (Sigma-Aldrich A2547, 1:100 dilution). Negative controls were included using isotype-matched control antibodies (Abcam). The severity of the pathologic changes was evaluated using the area of the neointimal hyperplasia lesion between the lumen and the vessel wall.

## Cell Culture

Male mice aged 6 to 8 weeks were euthanized by cervical dislocation. The bone marrow was isolated from the femur and tibia, filtered through a 70-μm nylon cell strainer, and dissociated in red-blood-cell lysis buffer. Purified cells were cultured in Dulbecco's Modified Eagle Medium containing 10% fetal bovine serum (all from Gibco, Gaithersburg, MD) and macrophage colony-stimulating factor (800 U/mL, Pepro Tech, Oak Park, CA) for another 4 days. Nonadherent cells were removed by aspiration and by washing with Dulbecco's Modified Eagle Medium, and ≈92% of the remaining

macrophages were CD11b-positive cells.[25] Descending thoracic aortas were harvested, cut into small pieces, and digested with type II collagenase (Worthington Biochemical Corporation) at 37°C for 1 hour. The cells were resuspended and cultured in Dulbecco's Modified Eagle Medium containing 20% fetal bovine serum and were used for 3 to 7 passages for the following experiments.

## Cell Proliferation and Migration Assay

Primary VSMCs were first cultured in a serum-free medium for 24 hours, treated with 20% CKD serum (derived from CKD mice, the serum was collected 3 weeks after right kidney removal) or normal medium for 48 hours, and subjected to Ki67 immunofluorescent staining for proliferation detection or Cell Counting Kit-8 (CCK-8) assay (Dojindo Laboratories, Kumamoto, Japan) to determine the total number. The Transwell assay was used to evaluate monocyte or VSMC migration in a Transwell chamber (8-μm pore size, Corning, NY). To evaluate monocyte migration, $10^5$ bone marrow–derived monocytes (in 200 μL of a serum-free medium) were cultured in the upper compartments of the Transwell migration chambers, while the primary VSMCs after processing (serum-free medium for 24 hours, 20% CKD serum medium stimulation for 48 hours) were cultured in the lower compartments. In another experiment to evaluate VSMC migration, VSMCs from *NLRP3*$^{fl/fl}$ or *NLRP3*$^{SMC\ KO}$ mice were treated with serum-free medium for 24 hours and 20% CKD serum or normal medium for 48 hours. Thereafter, $2\times10^4$ cells (in 200 μL of a serum-free medium) were cultured in the upper compartments, while normal medium in the lower compartments was used as a chemoattractant. Cells on the filter were removed after 24 hours (bone marrow–derived monocytes) or 6 hours (VSMCs), and the cells in the bottom chamber were fixed and stained with 0.2% crystal violet. The number of cells that migrated across the filter was counted in 5 random fields using a fluorescence microscope.

## Enzyme-Linked Immunosorbent Assay

Levels of IL-1β (EMC101b.48; NeoBioscience, Shenzhen, China), IL-4 (ADI-900-043; ENZO, NY), IL-6 (EMC004.48; NeoBioscience), IL-10 (BGK18893; Biogems, Westlake Village, CA), tumor necrosis factor (TNF)-α (EMC102a.96, NeoBioscience), interferon-γ (CMK0016; Jiamay Biotech, Beijing, China), macrophage colony-stimulating factor (EMC021.96; NeoBioscience), high mobility group box 1 (HMGB1, CSB-E08225m; Cusab, Wuhan, China), and transforming growth factor (TGF)-β (BGK04202; Biogems) in serum from CKD and sham mice were measured using commercially available kits according to the manufacturers' instructions. Absorbance was recorded using a microplate reader (Thermo Scientific, Helsinki, Finland) at 450 nm.

## Flow Cytometry

After culturing in serum-free medium for 24 hours, primary VSMCs from *NLRP3*$^{fl/fl}$ or *NLRP3*$^{SMC\ KO}$ mice were treated with 20% CKD serum for 48 hours. Then VSMCs were collected for Annexin V/PI staining (BD Biosciences, San Jose, CA) to quantify VSMC apoptosis or injected intraperitoneally ($10^5$ cells per C57BL/6 mice). Twelve hours later, the peritoneal lavage fluid was collected for flow cytometry. The following fluorochrome-conjugated antibodies were used: F4/80-fluorescein isothiocyanate (eBioscience 11-4801-82, 1:50 dilution), MHC II-PE (BD Biosciences 553566, 1:50 dilution), CD40-PerCP Cy5.5 (Biolegend 124623, 1:50 dilution), and CD80-PE Cy7 (Biolegend 104733, 1:50 dilution).

## Statistical Analysis

Data are presented as mean±SD. The unpaired Student *t* test was used to evaluate the differences between 2 individual experimental groups. Multiple comparisons were performed with 1-way ANOVA where appropriate. All data were analyzed using Prism 5.0 (GraphPad Software, Inc, San Diego, CA). $^*P<0.05$ was considered statistically significant. Results are representative of at least 3 independent experiments.

# Results

## NLRP3 Is Upregulated During CKD-Related AVF Failure

In order to examine the role of NLRP3 inflammasome signaling in CKD-related AVF failure, first, we detected NLRP3 expression in the outflow vein of occluded AVFs from patients with CKD, while great saphenous vein samples without varicosity were used as a control. Hematoxylin and eosin staining showed that significant stenosis existed in the occluded AVFs (Figure 1A). NLRP3 protein expression was significantly higher in the occluded AVFs than in the common great saphenous vein (Figure 1B). The mouse AVF model was obtained by an end-to-side ligation of the jugular vein to the carotid artery in 5 of 6 nephrectomy-induced CKD mice or sham control mice (Figure S2A and S2B); the venous outflow tract proximal to the anastomosis was harvested on POD 21 (Figure S2C). Hematoxylin and eosin and Elastica van Gieson staining indicated that the neointimal/lumen ratio of the AVF outflow vein from CKD mice was significantly higher than that of sham mice (Figure 1C and 1D). Co-staining for

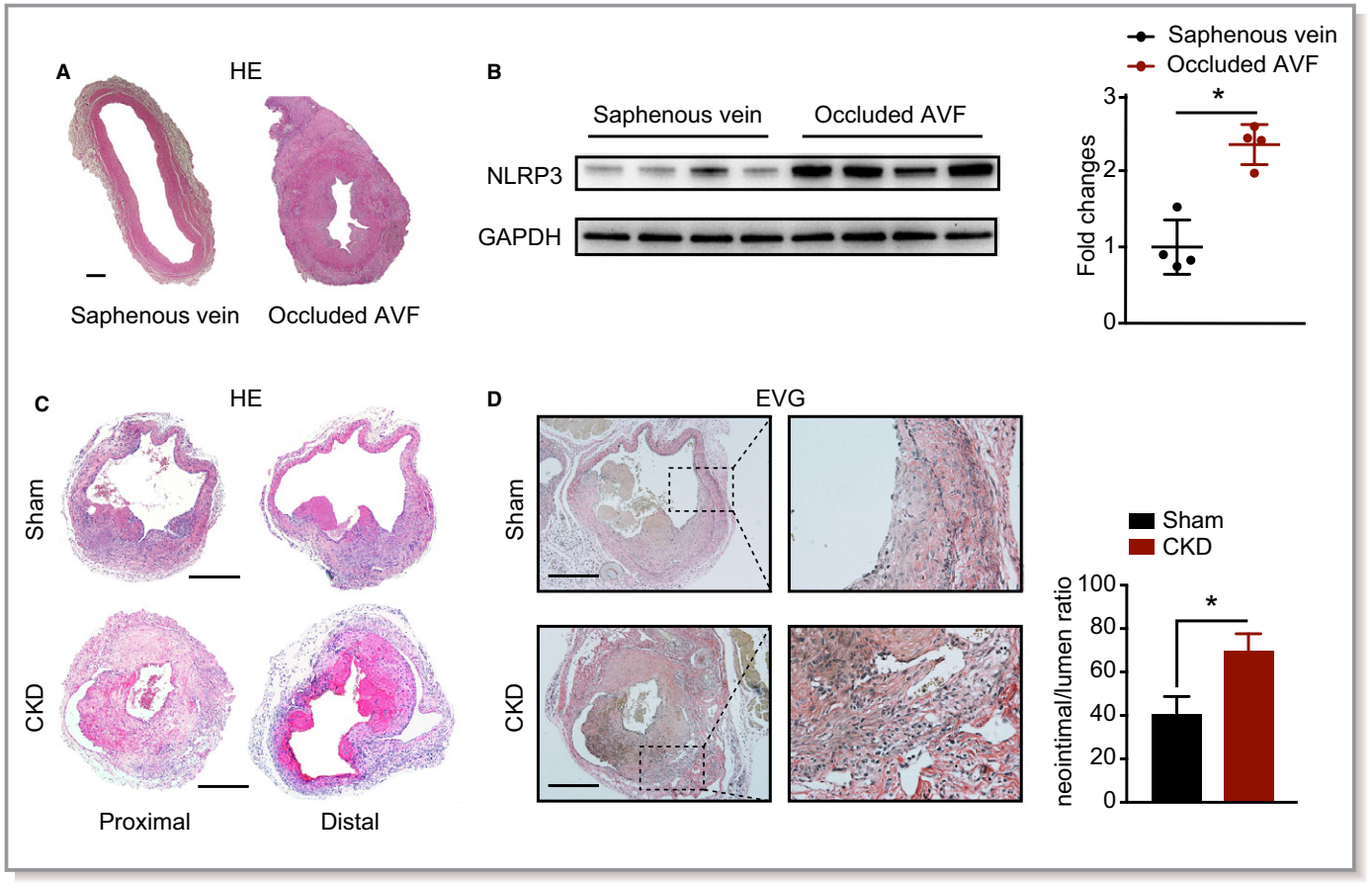


**Figure 1.** NLRP3 is upregulated in CKD-related AVF failure. **A**, HE staining of sections from human great saphenous vein or occluded AVFs. **B**, NLRP3 protein levels in a human great saphenous vein and occluded AVFs were determined using Western blot analysis (n=4 per group). Quantification is shown on the right. **C**, HE staining of outflow veins from the sham mice or CKD mice 3 wks after AVF construction. **D**, EVG staining of outflow veins (left) from the sham mice or CKD mice 3 wks after AVF construction. The severity of intimal hyperplasia was quantified as the neointimal/lumen ratio (n=6 per group, right). **E**, Immunofluorescence staining for CNN1 (green) and PCNA (red) was performed in outflow veins from the sham mice or CKD mice 3 wks after AVF construction. **F**, The counts (left) and proportion (right) of PCNA-positive VSMCs were calculated. **G**, *NLRP3* mRNA expression was measured by qPCR in the outflow vein of the AVFs from the sham or CKD mice; the contralateral jugular vein was used as a control (n=4 at each time point per group). Scale bars: 100 μm. **P*<0.05; ns, not statistically significant; data were analyzed by the unpaired *t* test. AVF indicates arteriovenous fistula; CKD, chronic kidney disease; CNN1, calponin 1; EVG, Elastica van Gieson; HE, hematoxylin and eosin; mRNA, messenger RNA; NLRP3, nucleotide-binding oligomerization domain-like receptor protein 3; PCNA, proliferating cell nuclear antigen; qPCR, quantitative real-time polymerase chain reaction; VSMC, vascular smooth muscle cell.

CNN1 (green) and PCNA (red) was used to quantify the proliferation of VSMCs in the outflow vein, and compared with the sham mice, the CKD mice had a much higher rate of PCNA-positive VSMCs (Figure 1E and 1F). When the contralateral internal jugular vein served as the control, in response to surgery, *NLRP3* mRNA expression of sham mice with AVF changed in a time-dependent manner, as *NLRP3* was increased in the mRNA level on POD 7, 14, and 21 but tended to normalize in the convalescent stage until POD 28. However, in AVFs from CKD mice, there was a more pronounced increase of NLRP3 (Figure 1G). These results indicated that NLRP3 signaling was upregulated during CKD-related AVF failure.

## VSMCs Express NLRP3 in Neointimal Lesions Induced by AVF

Given that NLRP3 was upregulated in the outflow vein upon CKD-related AVF failure, an immunofluorescence experiment was performed to determine the cell type(s) that NLRP3 was primarily localized in. After co-staining α-SMA, CNN1, or CD68 with NLRP3, we found that the increase of NLRP3 expression was primarily localized in the α-SMA-positive and CNN1-positive neointimal VSMCs (Figure 2A and 2B). A similar result was verified in the mouse outflow vein on POD 14 after AVF creation. In human samples, the contractile proteins α-SMA and SM22α were downregulated, while the synthetic protein,

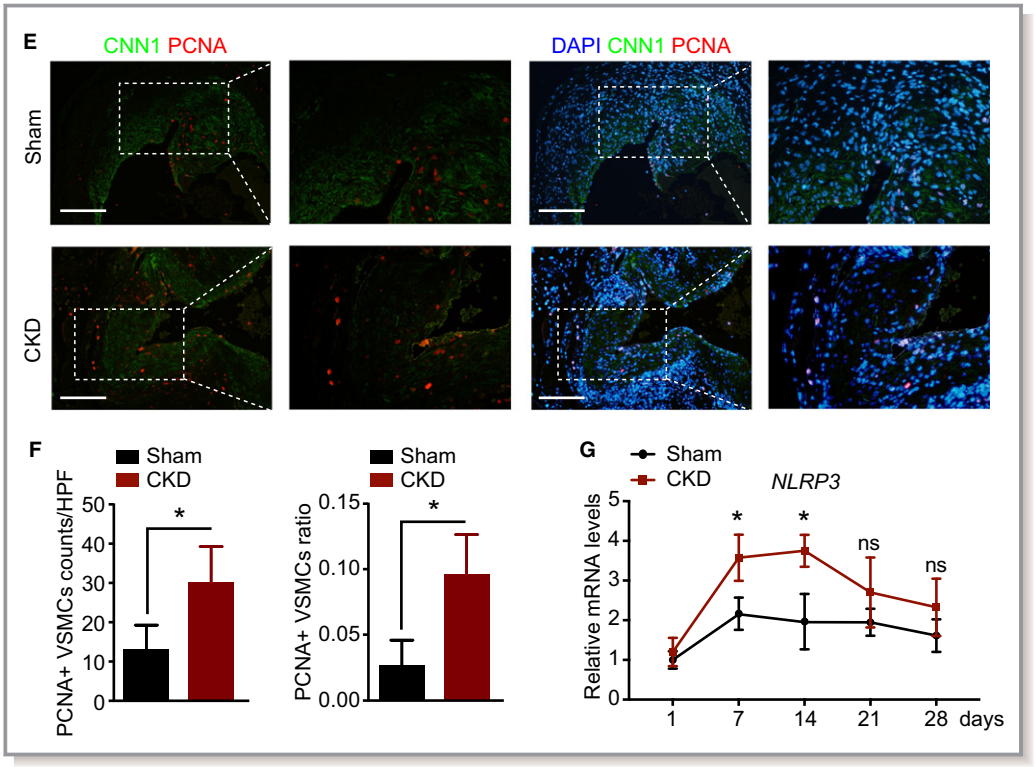


**Figure 1.** Continued

OPN, was upregulated, indicating that VSMCs differentiated into synthetic phenotype in AVF failure (Figure 2C). The same VSMC phenotypic transformation was also found in mice (Figure 2D). In order to confirm the activation of NLRP3 signaling in VSMCs in vitro, we treated primary VSMCs with sham or CKD mice serum. We observed an obvious upregulation in *NLRP3* mRNA levels (Figure 2E) and a reduction in the contractile proteins α-SMA and SM22α, while the OPN level was increased simultaneously (Figure 2F). To determine the critical factors in CKD mice serum that contribute to the overexpression of NLRP3 in VSMCs, serum from CKD or sham mice was analyzed using enzyme-linked immunosorbent assay. The results showed that levels of IL-1β, IL-6, IL-10, TNF-α, macrophage colony-stimulating factor, HMGB1, and TGF-β were higher in the serum of CKD mice than in that of sham mice (Figure S3A). *NLRP3* mRNA was found to be upregulated in VSMCs after TNF-α, macrophage colony-stimulating factor, and TGF-β stimulation according to the qPCR assay (Figure S3B). However, the role of the NLRP3 signaling pathway in VSMCs and its effect on AVF failure was still unknown.

## Smooth Muscle–Specific Deletion of NLRP3 Attenuates Outward IH Despite CKD

In order to verify the role of NLRP3 in CKD-related AVF failure, we obtained smooth-muscle-specific knockout NLRP3 ($NLRP3^{SMC\ KO}$) mice by crossbreeding $SM22\alpha\text{-}CreER^{T2}$ and $NLRP3^{fl/fl}$ mice (Figure 3A and 3B; Figure S4), and $NLRP3^{fl/fl}$ mice that were not introduced to Cre recombinase were used as littermate controls. AVF was established after CKD induction in $NLRP3^{SMC\ KO}$ and $NLRP3^{fl/fl}$ mice. Blood urea nitrogen, serum creatinine, body weight, blood pressure, and heart rate of $NLRP3^{SMC\ KO}$ and $NLRP3^{fl/fl}$ mice were measured on POD 21, and there was no statistical significance between the 2 groups (Figure S5A and S5B). The outflow veins obtained on POD 21 were examined for morphological changes. Hematoxylin and eosin and Elastica van Gieson staining indicated that the neointimal/lumen ratio was significantly lower in the outflow vein of $NLRP3^{SMC\ KO}$ mice than in $NLRP3^{fl/fl}$ littermates (Figure 3C and 3D). The total mRNA levels of PCNA in the outflow veins were measured at different time points (Figure S6A), and we found that the difference was more significant at 3 weeks. Therefore, the CNN1-positive and PCNA-positive indexes were used to quantify the proliferation of VSMCs in the outflow veins; compared with the $NLRP3^{fl/fl}$ mice, the $NLRP3^{SMC\ KO}$ mice had a much lower rate of PCNA-positive VSMCs at 3 weeks (Figure 3E and 3F). Finally, qPCR showed an upregulation of the VSMC marker, $SM22\alpha$ and a downregulation of OPN (Figure 3G). Therefore, the smooth muscle-specific deletion of NLRP3 significantly inhibited VSMC proliferation, and decreased the pro-inflammatory response and constrictive remodeling.

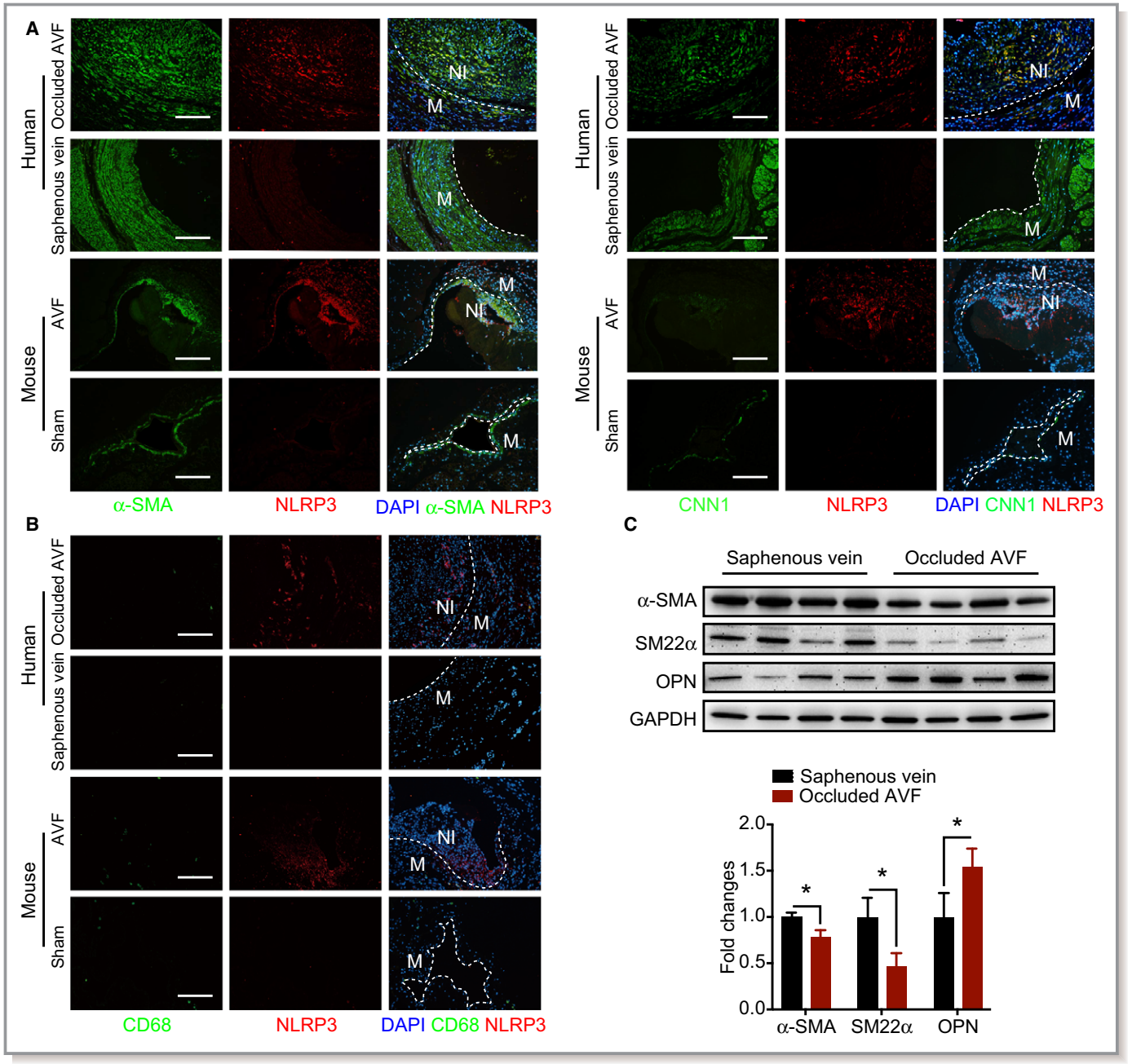


**Figure 2.** VSMCs express NLRP3 in neointimal lesions induced by AVF. **A**, Immunofluorescence staining for α-SMA (green) with NLRP3 (red) (left) and CNN1 (green) with NLRP3 (red) (right) were performed to determine NLRP3 localization of sections from occluded AVFs of humans and CKD mice 2 wks following AVF creation; a normal human great saphenous vein and the contralateral intact jugular vein of CKD mice served as controls. **B**, Immunofluorescence staining for CD68 (green) with NLRP3 (red) was also performed to determine NLRP3 localization of sections from occluded AVFs of humans and CKD mice 2 wks following AVF creation. **C**, Western blot analysis of α-SMA, SM22α and OPN protein levels in the human great saphenous vein and occluded AVF (n=4 per group). Quantification is shown at the bottom. **D**, mRNA expression levels of α-*SMA, SM22α*, and *OPN* in outflow veins from the sham mice or CKD mice 3 wks after AVF construction. **E**, In vitro mRNA expression levels of *NLRP3* in primary VSMCs from WT mice (VSMCs were harvested after 24 h starvation and 24 h 20% sham mice serum or CKD mice serum stimulation; VSMCs without stimulation were used as a control and measured by qPCR. **F**, In vitro mRNA expression levels of α-*SMA*, *SM22α*, and *OPN* in primary VSMCs from WT mice (VSMCs were harvested after 24 h starvation and 48 h 20% sham mice serum or CKD mice serum stimulation; VSMCs without stimulation were used as a control and measured by qPCR. Scale bars: 20 μm. **P*<0.05; ns, not statistically significant; data were analyzed by the unpaired *t* test. α-SMA indicates α-smooth muscle actin; AVF, arteriovenous fistula; CKD, chronic kidney disease; CNN1, calponin 1; DAPI, 4′,6-diamidino-2-phenylindole; mRNA, messenger RNA; NLRP3, nucleotide-binding oligomerization domain-like receptor protein 3; OPN, osteopontin; qPCR, quantitative real-time polymerase chain reaction; SM22α, smooth muscle protein 22 α; VSMC, vascular smooth muscle cell; WT, wild-type.

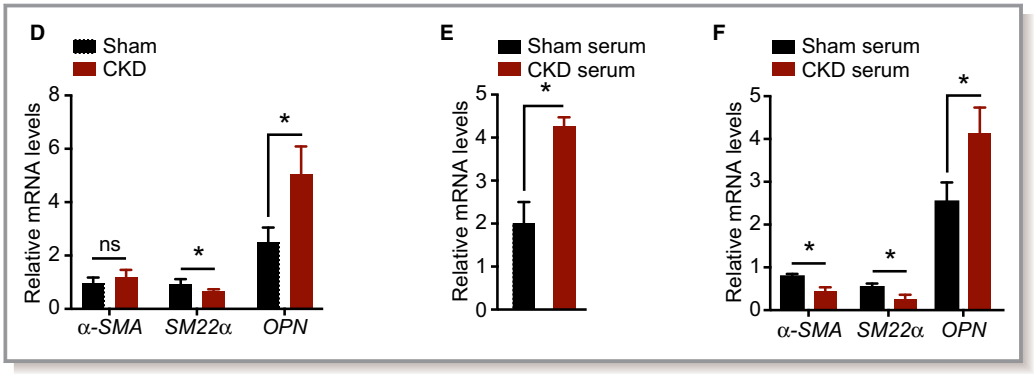


**Figure 2.** Continued

## NLRP3 Deficiency Inhibits VSMC Proliferation, Migration, and Phenotypic Switching

In order to examine whether *NLRP3* gene deletion affects VSMC proliferation and migration in vitro, primary VSMCs from *NLRP3*$^{fl/fl}$ and *NLRP3*$^{SMC\ KO}$ mice were treated with CKD serum. VSMC proliferation was evaluated by measuring Ki67 incorporation. After CKD serum stimulation, *NLRP3*-deficient VSMCs incorporated less Ki67, whereas *NLRP3*$^{fl/fl}$ VSMCs incorporated more Ki67, indicating that NLRP3 facilitates a proliferative response upon CKD serum stimulation (Figure 4A). The CCK-8 was used to detect the total number of VSMCs after CKD serum stimulation. We found that the number of *NLRP3*-deficient VSMCs slightly decreased, but there was no statistical significance after 48 hours. However, after 96 hours, the number of *NLRP3*-deficient VSMCs was significantly lower than those in the controls (Figure 4B). Transwell chamber migration assay was performed to evaluate VSMC migration. After CKD serum stimulation, fewer *NLRP3*-deficient VSMCs, compared with *NLRP3*$^{fl/fl}$ VSMCs, migrated through the membrane (Figure 4C). Flow cytometry analysis with Annexin V/PI staining was used to quantify VSMC apoptosis upon CKD serum stimulation; we found no significant difference between *NLRP3*-deficient VSMCs and *NLRP3*$^{fl/fl}$ VSMCs (Figure 4D). In order to examine whether *NLRP3* gene deletion affects VSMC phenotypic switching after CKD serum stimulation, VSMC marker genes were examined by Western blot; SM22α was found to be significantly higher, while OPN was downregulated in *NLRP3*-deficient VSMCs (Figure 4E). These results indicate that NLRP3 ablation inhibits VSMCs proliferation, migration, and phenotypic transformation after CKD serum stimulation.

## NLRP3 Deficiency Reduces Crosstalk Between VSMCs and Macrophages

Because VSMCs are a source and target of cytokines, VSMCs may serve as local propagators of the immune response in AVF failure.[3] To determine whether *NLRP3*-deficient VSMCs responded to stimuli more robustly than controls, primary VSMCs from *NLRP3*$^{fl/fl}$ mice and *NLRP3*$^{SMC\ KO}$ mice were treated with the CKD serum. Expression levels of *IL-1*α, *IL-1*β, *IL-6*, *Tnf-*α, *C-C Motif Chemokine Ligand 2* (*Ccl2*), *C-X-C Motif Chemokine Ligand 12* (*Cxcl12*), and *C-X3-C Motif Chemokine Ligand 1* (*Cx3cl1*) were determined by qPCR, and the results demonstrated that all potent proinflammatory and chemotactic cytokines were significantly decreased in VSMCs explanted from *NLRP3*-deficient mice compared with the controls (Figure 5A). The VSMCs released inflammatory cytokines that stimulated monocytes activation to promote vein vascular remodeling. In order to evaluate whether NLRP3 deficiency in VSMCs attenuated macrophage recruitment, we cultured the bone marrow–derived monocytes in the upper compartments of Transwell migration chambers, while the CKD serum-treated primary VSMCs from *NLRP3*$^{fl/fl}$ or *NLRP3*$^{SMC\ KO}$ mice in the lower compartments as a chemoattractant. The results showed a reduction of monocyte chemotaxis in VSMCs from *NLRP3*$^{SMC\ KO}$ mice compared with that from *NLRP3*$^{fl/fl}$ mice (Figure 5B). To determine the effects of *NLRP3*-deficient VSMCs on inflammatory cells in vivo, we injected the CKD serum-treated VSMCs into C57BL/6 mice intraperitoneally. The peritoneal lavage fluid was collected for flow cytometry 12 hours later. The counts and proportion of macrophages (F4/80+ and MHC II+), B cells (F4/80− and MHC II+), and T cells/neutrophils (F4/80− and MHC II−) were calculated (Figure 5C and 5D). The activation of macrophages was assayed by expression of MHC II, CD40, and CD80 (Figure 5E). The results revealed that *NLRP3*-deficient VSMCs, compared with *NLRP3*$^{fl/fl}$ VSMCs, mainly reduced macrophage chemotaxis and activation (MHC II and CD40). Therefore, we confirmed that NLRP3 in VSMCs promoted inflammatory factor expression and macrophage recruitment in VSMCs.

## NLRP3 Deficiency Blocks VSMCs Phenotypic Transformation Via Smad2/3 Suppression

NLRP3 has been reported to affect caspase-1 and IL-1β expression in VSMCs and regulate Smad2/3 signaling in non-

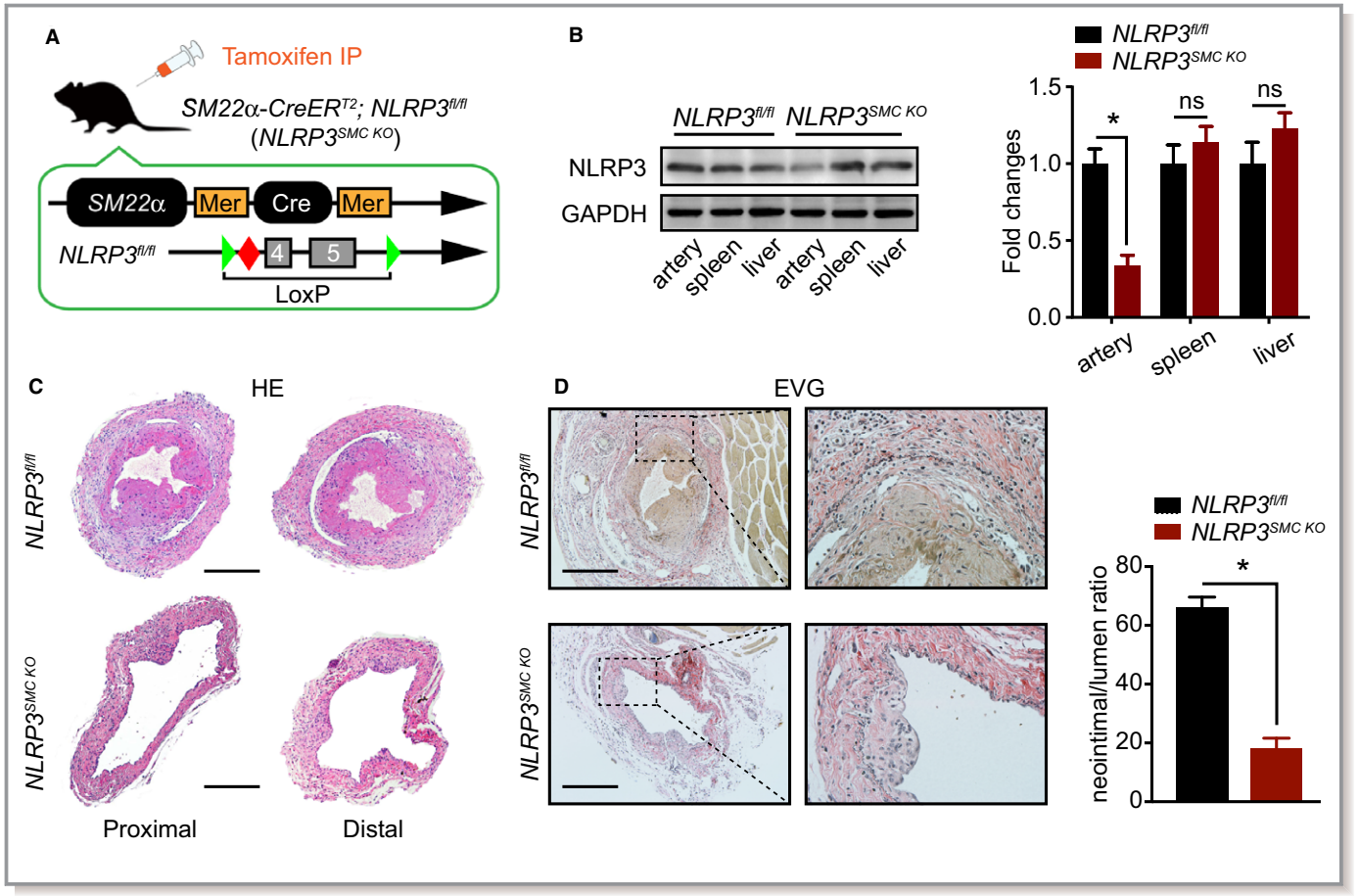


**Figure 3.** Smooth muscle–specific deletion of NLRP3 attenuates intimal hyperplasia. **A**, Schematic illustration of *NLRP3*$^{SMC\ KO}$ mice generation. **B**, Western blot analysis of NLRP3 protein levels in different tissues of *NLRP3*$^{fl/fl}$ and *NLRP3*$^{SMC\ KO}$ mice. Quantification is shown on the right. **C**, HE staining of the outflow veins from CKD *NLRP3*$^{fl/fl}$ and CKD *NLRP3*$^{SMC\ KO}$ mice 3 wks after AVF construction. **D**, EVG staining of the outflow veins (left) from CKD *NLRP3*$^{fl/fl}$ and CKD *NLRP3*$^{SMC\ KO}$ mice 3 wks after AVF construction. The severity of intimal hyperplasia was quantified as the neointimal/lumen ratio (n=5–6 per group, right). **E**, Immunofluorescence staining for CNN1 (green) and PCNA (red) was performed in outflow veins from CKD *NLRP3*$^{fl/fl}$ and CKD *NLRP3*$^{SMC\ KO}$ mice 3 wks after AVF construction. **F**, The counts (left) and proportion (right) of PCNA-positive VSMCs were calculated. **G**, α-*SMA*, *SM22*α, and *OPN* mRNA expressions were measured by qPCR in the outflow veins of the AVFs from CKD *NLRP3*$^{fl/fl}$ and CKD *NLRP3*$^{SMC\ KO}$ mice 3 wks after AVF construction; the contralateral jugular vein was used as a control (n=5–6 per group). Scale bars: 100 μm. **P*<0.05; ns, not statistically significant; data were analyzed by the unpaired *t* test. AVF indicates arteriovenous fistula; CKD, chronic kidney disease; CNN1, calponin 1; EVG, Elastica van Gieson; HE, hematoxylin and eosin; mRNA, messenger RNA; NLRP3, nucleotide-binding oligomerization domain-like receptor protein 3; *NLRP3*$^{SMC\ KO}$, smooth muscle–specific knockout nucleotide-binding oligomerization domain-like receptor protein 3; OPN, osteopontin; PCNA, proliferating cell nuclear antigen; qPCR, quantitative real-time polymerase chain reaction; SM22α, smooth muscle protein 22 α; VSMC, vascular smooth muscle cell; α-SMA, α-smooth muscle actin.

VSMCs. In order to ascertain how NLRP3 regulates the phenotypic switching process of VSMCs, we detected both pathways in human specimens, and observed that both were activated in AVFs (Figure 6A). In vitro, both pathways were similarly suppressed in *NLRP3*-deficient VSMCs after CKD serum stimulation (Figure 6B and 6C). The small-molecule inhibitors that block caspase-1/IL-1β or Smad2/3 signaling were used. We found that SIS3 (Smad3 inhibitor), but not VX-765 (caspase-1 inhibitor), significantly suppressed CKD serum-induced VSMC proliferation (Figure 6D) and migration (Figure 6E), showing that NLRP3 regulates VSMC proliferation and migration through Smad2/3 phosphorylation rather than through caspase-1/interleukin-1β signaling. Interestingly, MCC950, a diarylsulfonylurea-based compound reported as a highly specific NLRP3 inhibitor and considered to be an inflammasome-related pathway blocker,[26] also significantly attenuated VSMC proliferation (Figure 6D), migration (Figure 6E), and repressed Smad2/3 signaling (Figure S7), which might be related to its effect on ASC function.

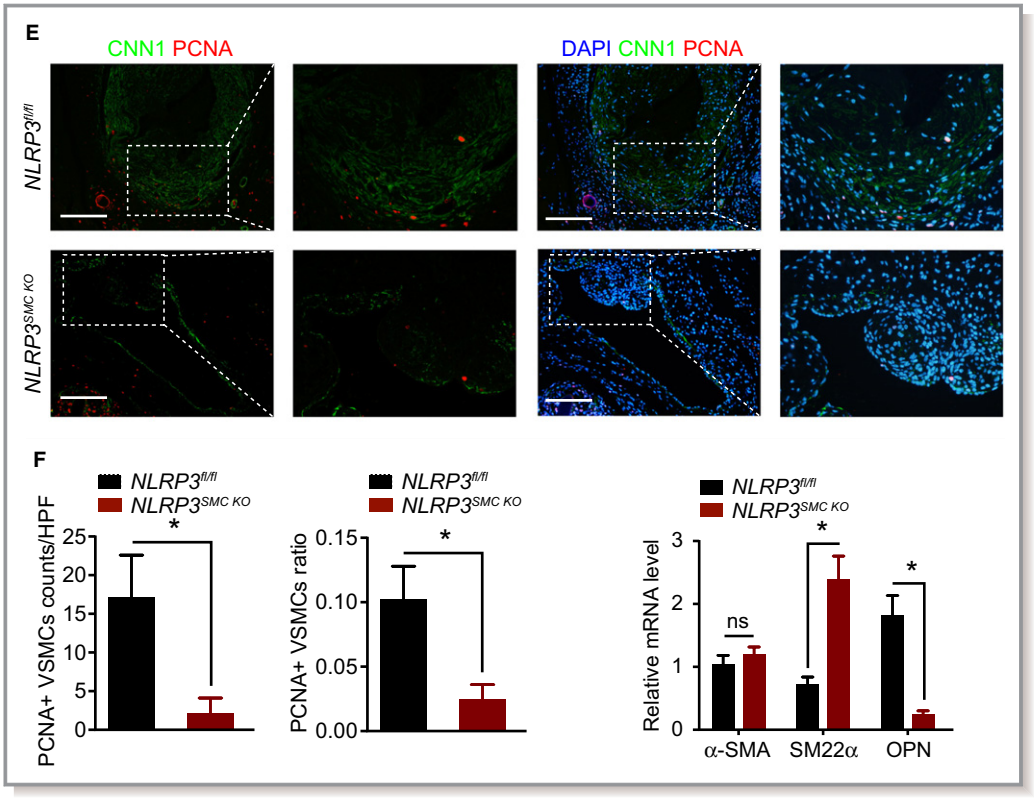


**Figure 3.** Continued

## NLRP3 Inhibitor MCC950 Attenuates IH Independent of Macrophages

In order to verify that MCC950 could reduce outflow vein IH induced by AVF surgery, 10 mg/kg of MCC950[26–28] or vehicle was administered every other day after AVF creation in CKD WT mice. Blood urea nitrogen, serum creatinine, body weight, blood pressure, and heart rate were measured on POD 21, and there was no statistical significance between the 2 groups (Figure S5C and S5D). The outflow veins harvested on POD 21 were examined for morphological changes. Compared with vehicle treatment, treatment with 10 mg/kg MCC950 significantly attenuated IH and the neointimal/lumen ratio in the outflow vein (Figure 7A and 7B). The total mRNA levels of *PCNA* (Figure S6B) and VSMC proliferation (Figure 7C and 7D) was also significantly reduced in the outflow vein of AVF from CKD WT mice treated with MCC950. Additionally, the MCC950 group showed higher levels of *SM22α* mRNA with lower expression of *OPN*, which meant that MCC950 reduced the VSMCs phenotypic switching in AVF worsened by CKD (Figure 7E). Given the clear inhibitory effects of MCC950 on macrophages, which may play a role in the improvement of AVF, we utilized clodronate liposomes[29] to eliminate the mononuclear macrophages in CKD WT mice (Figure S8), and with analogous results, MCC950 significantly attenuated IH and VSMCs phenotypic switching in the outflow veins of CKD WT mice in the presence of clodronate liposomes (Figure 7F through 7H). Generally, we concluded that MCC950 worked independently of macrophages.

## Discussion

The present study provides new insights, indicating that NLRP3 activation contributes to IH induced by AVF surgery and CKD. We observed that NLRP3 signaling was upregulated in the AVF failure period and that the increased NLRP3 was primarily localized in the neointima VSMCs. Thereafter, *NLRP3*$^{SMC\ KO}$ mice showed that smooth muscle–specific knockout NLRP3 attenuates AVF IH; inhibits VSMC phenotypic transformation, proliferation, and migration; and prevents macrophage recruitment by preventing VSMCs Smad2/3 phosphorylation. We finally discovered that MCC950 (a small-molecule inhibitor of NLRP3) administration resulted in tolerance to AVF-induced IH despite CKD.

Immunohistochemistry revealed that most neointimal cells in the neointima of outflow veins express α-SMA, thereby identifying these cells as SMCs, myofibroblasts, or "myofibroblast-like" cells.[30] Recent studies demonstrated dedifferentiated VSMCs, which expressed relatively low levels of ACTA2 (α-SMA) and CNN1, and little to no

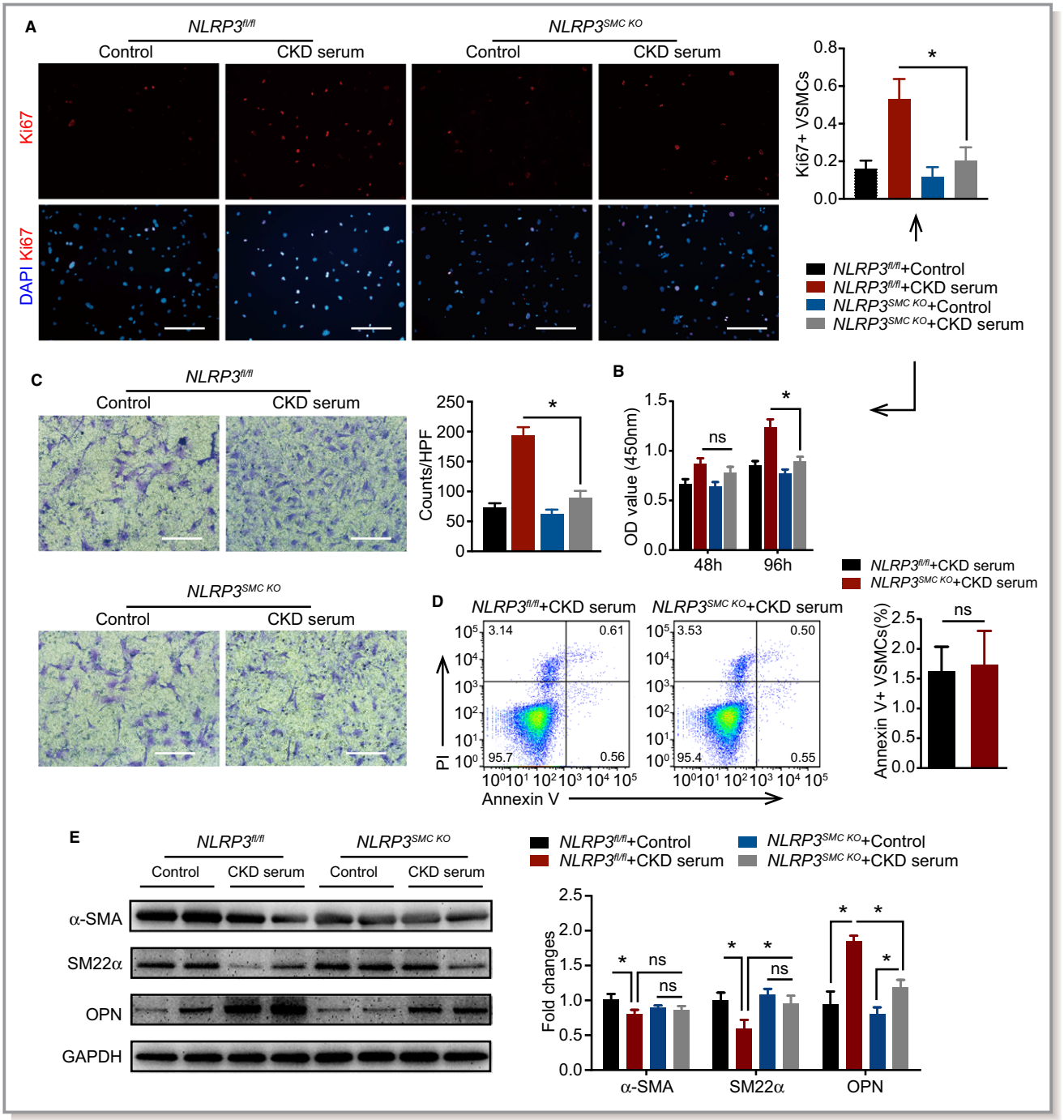


**Figure 4.** NLRP3 deficiency inhibits VSMCs proliferation, migration, and phenotypic switching. **A**, Immunofluorescence staining for Ki67 (red) to demonstrate the proliferation of primary VSMCs (left) from *NLRP3*$^{fl/fl}$ and *NLRP3*$^{SMC\ KO}$ mice after 24 h starvation and 48 h 20% CKD serum or normal medium stimulation. The proportions of Ki67-positive VSMCs were calculated (right). **B**, CCK-8 assay for the total number of VSMCs after 24 h starvation and 48 h/96 h 20% CKD serum or normal medium stimulation. **C**, The primary VSMCs of *NLRP3*$^{fl/fl}$ and *NLRP3*$^{SMC\ KO}$ mice were seeded on the Transwell dishes to perform migration assays. Cells migrating through the membrane were fixed after 6 h (left). The cell number per HPF was counted (right). **D**, Flow cytometry analysis for Annexin V/PI staining was used to quantify apoptosis of VSMCs from *NLRP3*$^{fl/fl}$ and *NLRP3*$^{SMC\ KO}$ mice after 24 h starvation and 48 h 20% CKD serum stimulation. Quantification is shown in the right. **E**, Western blot analysis of α-SMA, SM22α, and OPN protein levels in primary VSMCs from *NLRP3*$^{fl/fl}$ and *NLRP3*$^{SMC\ KO}$ mice after 24 h starvation and 48 h 20% CKD serum or normal medium stimulation. Quantification is shown on the right. Scale bars: 20 μm. **P*<0.05; ns, not statistically significant; data were analyzed by 1-way ANOVA (**A**, **B**, **C**, and **E**) or the unpaired *t* test (**D**). α-SMA indicates α-smooth muscle actin; ANOVA, analysis of variance; CCK-8, cell counting kit-8; CKD, chronic kidney disease; HPF, high-power field; NLRP3, nucleotide-binding oligomerization domain-like receptor protein 3; *NLRP3*$^{SMC\ KO}$, smooth-muscle-specific knockout nucleotide-binding oligomerization domain-like receptor protein 3; OD, optical density; OPN, osteopontin; SM22α, smooth muscle protein 22 α; VSMC, vascular smooth muscle cell.

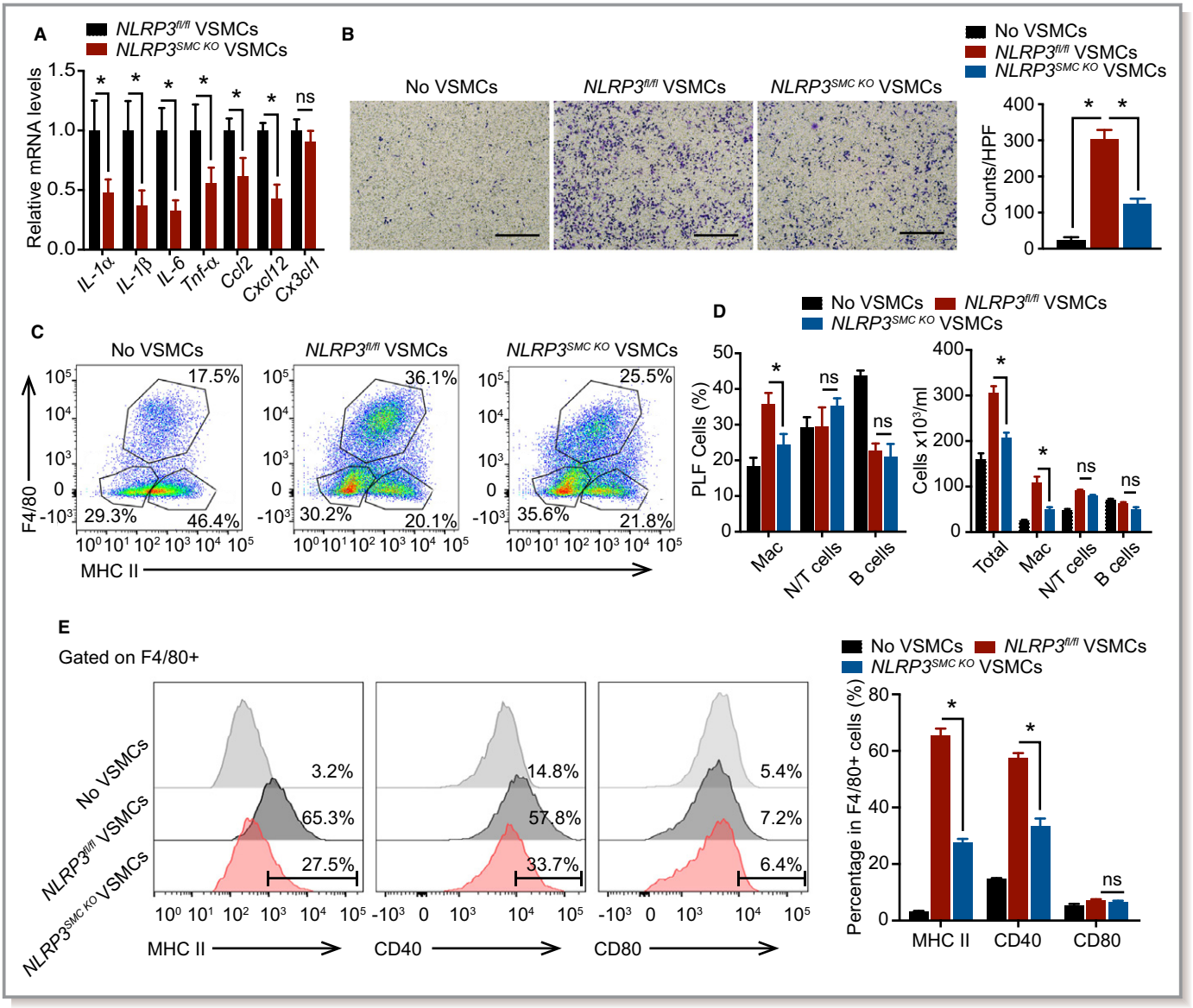


**Figure 5.** NLRP3 deficiency reduces crosstalk between VSMCs and macrophages. **A**, mRNA expression levels of *IL-1α, IL-1β, IL-6, Tnf-α, Ccl2, Cxcl12*, and *Cx3cl1* in primary VSMCs from *NLRP3*$^{fl/fl}$ and *NLRP3*$^{SMC\ KO}$ mice after 24 h starvation and 48 h 20% CKD serum stimulation. **B**, Bone marrow–derived monocytes from WT mouse were seeded on Transwell dishes to perform migration assays. Primary VSMCs from *NLRP3*$^{fl/fl}$ and *NLRP3*$^{SMC\ KO}$ mice after 24 h starvation and 48 h 20% CKD serum stimulation were used as a chemoattractant. Cells migrating through the membrane were fixed after 24 h (left) and the cell number per HPF was counted (right). **C**, Primary VSMCs from *NLRP3*$^{fl/fl}$ or *NLRP3*$^{SMC\ KO}$ mice after 24 h starvation and 48 h 20% CKD serum stimulation were harvested and then injected into WT mice intraperitoneally. The peritoneal lavage fluid was collected for flow cytometry after 12 h. **D**, The proportion (left) and estimated counts (right) of macrophages (F4/80+, MHC II+), B cells (F4/80−, MHC II+), and T cells/neutrophils (F4/80− and MHC II−) were calculated. **E**, The activation of macrophages was assayed by expressions of MHC II, CD40, and CD80. Quantification is shown on the right. Scale bars: 20 μm. **P*<0.05; ns, not statistically significant; data were analyzed by the unpaired *t* test. CCL2 indicates C-C Motif Chemokine Ligand 2; CKD, chronic kidney disease; CX3CL1, C-X3-C Motif Chemokine Ligand 1; CXCL12, C-X-C Motif Chemokine Ligand 12; IL, interleukin; Mac, macrophages; mRNA, messenger RNA; NLRP3, nucleotide-binding oligomerization domain-like receptor protein 3; *NLRP3*$^{SMC\ KO}$, smooth-muscle-specific knockout nucleotide-binding oligomerization domain-like receptor protein 3; N/T, neutrocytes or T cells; PLF, peritoneal lavage fluid; TNF, tumor necrosis factor; VSMC, vascular smooth muscle cell; WT, wild-type.

expression of myosin heavy chain 11 (MYH11), contributing to neointimal hyperplasia in AVF, through VSMC lineage tracing reporter mouse (Myh11-Cre/ERT2-mTmG).[5] Here, we proved that NLRP3 protein is mainly localized in α-SMA-positive and CNN1-positive cells. Additionally, the systemic effects of CKD play a significant role in AVF failure.[31] The

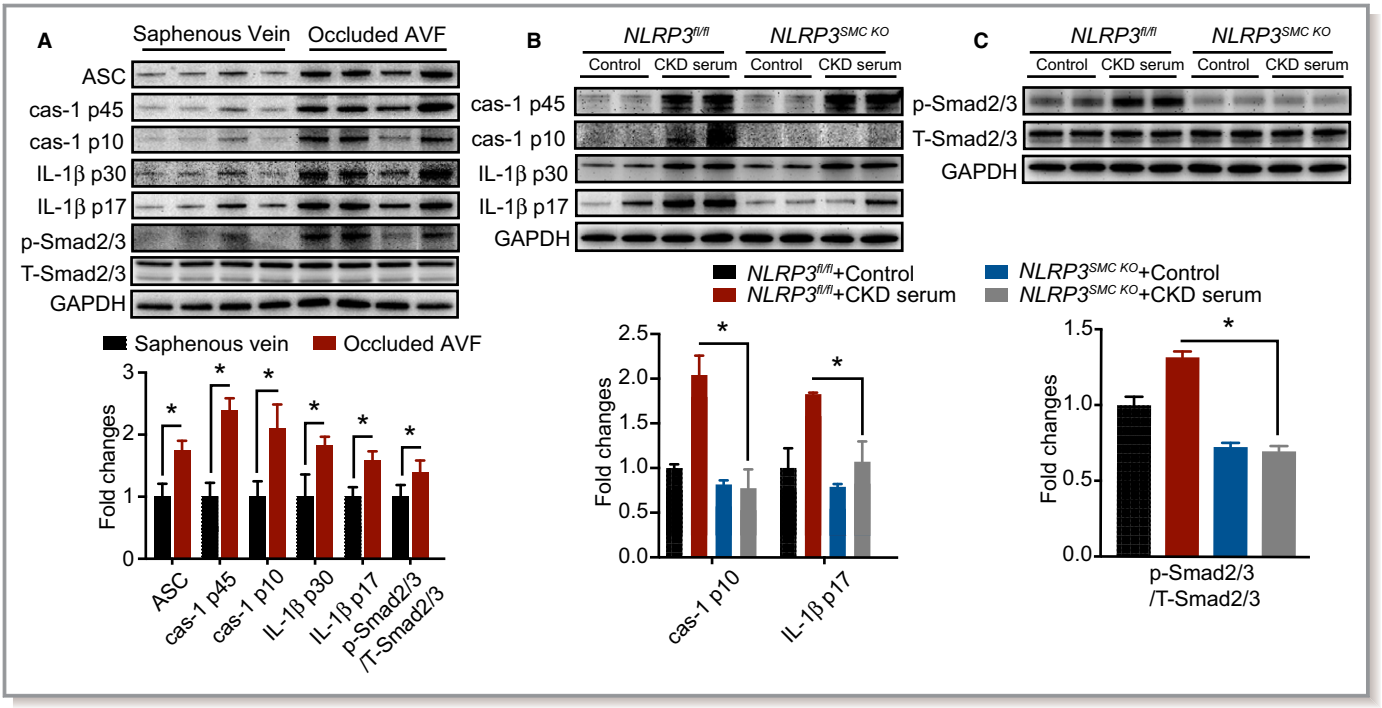


**Figure 6.** NLRP3 deficiency blocks VSMC phenotypic transformation via SMAD2/3 suppression. **A**, ASC, caspase-1, IL-1β, and Smad2/3 protein levels in the great saphenous vein and occluded AVFs were determined using Western blot analysis (n=4 per group). Quantification is shown at the bottom. **B**, In vitro, ASC, caspase-1, IL-1β protein levels in primary VSMCs from *NLRP3*$^{fl/fl}$ and *NLRP3*$^{SMC\ KO}$ mice (VSMCs were harvested after 24 h starvation and 48 h 20% CKD serum or normal medium stimulation) were determined using Western blot analysis. Quantification is shown at the bottom. **C**, Smad2/3 protein levels in primary VSMCs from *NLRP3*$^{fl/fl}$ and *NLRP3*$^{SMC\ KO}$ mice (VSMCs were harvested after 24 h starvation and 48 h 20% CKD serum or normal medium stimulation) was determined using Western blot analysis. Quantification is shown at the bottom. **D**, Immunofluorescence staining for Ki67 (red) was used to demonstrate the proliferation of primary VSMCs (left) from WT mice after 24 h starvation and 48 h 20% CKD serum stimulation in the presence of MCC950 (50 μmol/L), VX-765 (20 μmol/L), and SIS3 (3 μmol/L). The proportions of Ki67-positive VSMCs were calculated (right). **E**, Transwell assays were used to evaluate the migration of primary VSMCs (left) from WT mice after 24 h starvation and 48 h 20% CKD serum stimulation in the presence of MCC950 (50 μmol/L), VX-765 (20 μmol/L), and SIS3 (3 μmol/L), and the cell number per HPF was counted (right). Scale bars: 20 μm. *$P$<0.05; ns, not statistically significant; data were analyzed by the unpaired $t$ test (**A**, **D**, and **E**) or 1-way ANOVA (**B** and **C**). ASC indicates adaptor apoptosis-associated speck-like protein containing a caspase-recruitment domain; AVF, arteriovenous fistula; CKD, chronic kidney disease; DAPI, 4′,6-diamidino-2-phenylindole; HPF, high-power field; IL, interleukin; NLRP3, nucleotide-binding oligomerization domain-like receptor protein 3; *NLRP3*$^{SMC\ KO}$, smooth muscle–specific knockout nucleotide-binding oligomerization domain-like receptor protein 3; VSMC, vascular smooth muscle cell; WT, wild-type.

potential for successful outward remodeling and adequate maturation of a healthy vein may be hindered by CKD-induced vasculopathy, such as IH.[4] VSMCs cultured with CKD serum, compared with those cultured with sham serum, showed significantly increased migration. Moreover, mice with CKD had higher serum levels of OPN, which could stimulate VSMC migration.[6] Local mechanisms controlling VSMC migration and proliferation are important contributors to maturation failure.[32] Thus, we focused more on the function of VSMCs in CKD-related AVF.

Our study revealed the vital role of NLRP3 in AVF and verified its effect on AVF failure acceleration. We concluded that NLRP3 might play a crucial role in regulating Smad2/3 phosphorylation during CKD-related AVF failure. A previous study showed that the systematic knockout of caspase-1 could extenuate IH induced by carotid artery ligation in CKD.[33] This was consistent with our conclusion; our study also showed inhibitory effects on VSMC proliferation caused, to some extent, by caspase-1 inhibitor. However, our study showed that both caspase-1/IL-1β and Smad2/3 signaling were suppressed in *NLRP3*-deficient VSMCs, and CKD serum-induced VSMC proliferation and migration were more significantly suppressed by Smad3 inhibitor than caspase-1 inhibitor, suggesting that NLRP3 regulates the VSMC phenotypic switching process through Smad2/3 phosphorylation rather than through caspase-1/IL-1 signaling. Therefore, the suppression of inflammatory cells by the systematic knockout of caspase-1 should not be ignored.[10] A limitation of the present study is that we could not determine how NLRP3 regulates Smad2/3 phosphorylation in VSMC.

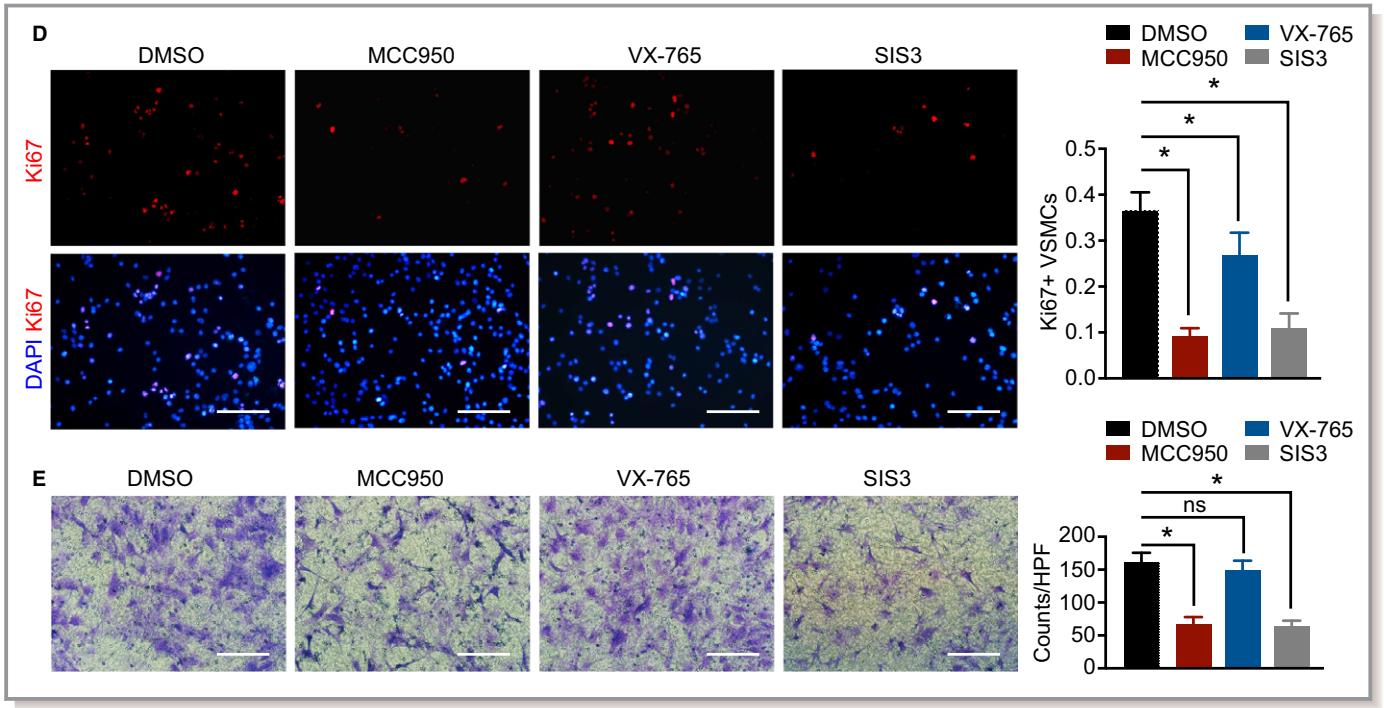


**Figure 6.** Continued

VSMCs in the vessel wall may serve as local propagators of the immune response.[3] Our study indicated that inflammatory factors were released in VSMCs treated with CKD serum. Crosstalk between VSMCs and monocytes ultimately induced IH, during which VSMCs secreted cytokines to activate monocytes, which, in turn, released more inflammatory factors acting on VSMCs.[3,34] Here, smooth muscle–specific knockout NLRP3 exhibited decreased levels of secretory markers, reduced secretion of inflammatory factors, and weakened monocyte-activating ability. The effects above could explain why smooth muscle–specific knockout NLRP3 was protective against AVF failure from CKD.

We found that the inflammasome inhibitor of NLRP3 also repressed Smad2/3 phosphorylation in VSMCs. Although some researchers believed the NLRP3 regulation of Smad2/3 signaling was independent of the inflammasome in fibroblasts, $ASC^{-/-}$ still significantly reduced Smad2/3 phosphorylation.[17] Both NLRP3 and ASC are needed for TGF-β1-mediated Smad2/3 phosphorylation in dendritic cells.[18] Although MCC950 does not affect NLRP3 or ASC expression, it can block NLRP3-induced ASC oligomerization,[26] which might be responsible for its suppression of Smad2/3 phosphorylation in VSMCs. Considering the notable inhibition of mononuclear macrophages by the NLRP3 blocker, MCC950, we aimed to ascertain its effects on VSMCs, since it seemed clear that it mitigated IH in AVF. Thus, we cleared the mononuclear macrophages by using clodronate liposomes and clarified that MCCC950 worked independently of macrophages.

Hyperglycemia,[35] hypertension,[36] calcification,[37] and inflammatory factors such as TNF-α[38] and HMGB1[39] have been reported to activate NLRP3-related signaling pathways in VSMCs. The mechanisms of NLRP3 upregulation in VSMCs during CKD-related AVF are unknown. Endothelial injury, hemodynamic changes, and inflammatory cell infiltration may all contribute to this pathology. The complex causes of AVF failure are related to systemic changes associated with CKD. Recent work has shown that cytokines implicated in IH formation, including IL-6, TGF-β1, and TNF-α, are increased in uremia.[40] These stressors have been shown to increase the levels of potent mitogens, in addition to the local inflammation and hypoxia that occur during AVF creation.[41] Our results showed that CKD mice serum, compared with sham mice serum, could further upregulate NLRP3 in VSMCs. We also found that several inflammatory factors, which were increased in the serum of CKD mice, could promote the expression of NLRP3 in VSMCs. Additionally, markers of oxidative damage and lipid peroxidation—8-hydroxy-20-deoxyguanosine, and 4-hydroxy-2-nonenal, whose effects are unknown—have also been identified in uremia.[40] Further study is needed to determine which factor is the most critical in VSMCs NLRP3 upregulation during CKD-related AVF.

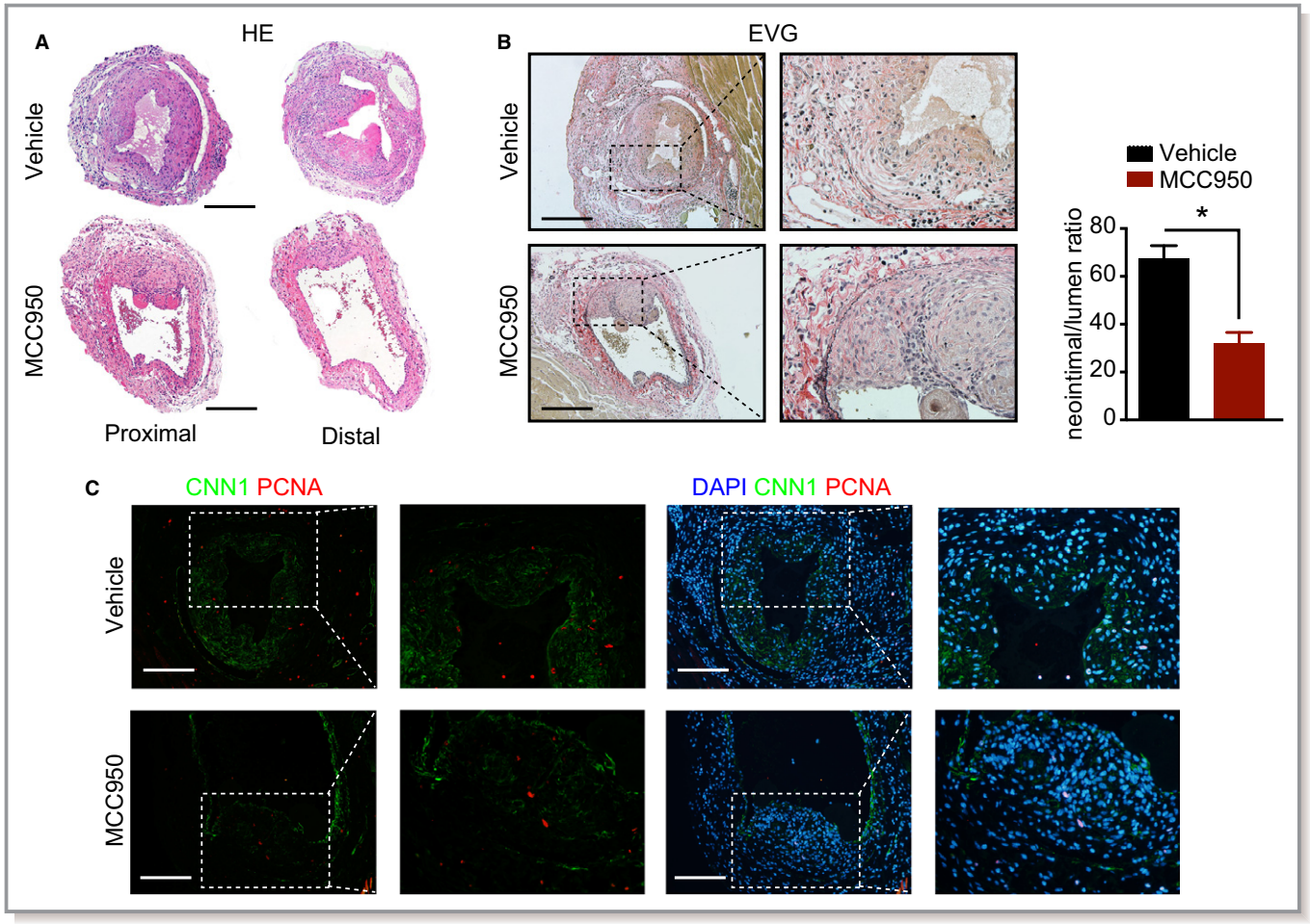


**Figure 7.** MCC950 attenuates intimal hyperplasia independent inflammatory cells. **A**, HE staining of the outflow vein from vehicle-treated and MCC950-treated CKD WT mice 3 wks after AVF construction. **B**, EVG staining of the outflow vein (left) from vehicle-treated and MCC950-treated CKD WT mice 3 wks after AVF construction. The severity of intimal hyperplasia was quantified as the neointimal/lumen ratio (n=6 per group, right). **C**, Immunofluorescence staining for CNN1 (green) and PCNA (red) was performed in outflow veins from vehicle-treated and MCC950-treated CKD WT mice 3 wks after AVF construction. **D**, The counts (left) and proportion (right) of PCNA-positive VSMCs were calculated. **E**, α-*SMA, SM22α,* and *OPN* mRNA expression was measured by qPCR in the outflow veins of the AVFs from vehicle-treated and MCC950-treated CKD WT mice 3 wks after AVF construction. **F**, HE staining of the outflow veins from vehicle-treated and MCC950-treated CKD WT mice in the presence of LC 3 wks after AVF construction. **G**, EVG staining of the outflow veins (left) from vehicle-treated and MCC950-treated CKD WT mice in the presence of LC 3 wks after AVF construction. The severity of intimal hyperplasia was quantified as the neointimal/lumen ratio (n=5–6 per group, right). **H**, α-*SMA, SM22α* and *OPN* mRNA expression was measured by qPCR in the outflow veins of the AVFs from vehicle-treated and MCC950-treated CKD WT mice in the presence of LC 3 wks after AVF construction. Scale bars: 100 μm. **P*<0.05; ns, not statistically significant; data were analyzed by the unpaired *t* test. α-SMA indicates α-smooth muscle actin; AVF, arteriovenous fistula; CKD, chronic kidney disease; CNN1, calponin 1; DAPI, 4′,6-diamidino-2-phenylindole; EVG, Elastica van Gieson; HE, hematoxylin and eosin; LC, clodronate liposomes; mRNA, messenger RNA; OPN, osteopontin; PCNA, proliferating cell nuclear antigen; qPCR, quantitative real-time polymerase chain reaction; SM22α, smooth muscle protein 22 α; VSMC, vascular smooth muscle cell; WT, wild-type.

The role of vascular outward remodeling in the AVF setting is often neglected. Adequate outward remodeling could preserve luminal caliber and may, therefore, be valuable for successful fistula maturation.[42] Although our study noted the inhibition of VSMCs phenotypic switching, proliferation, migration, and inflammatory mediator secretion in NLRP3 deficiency, and all of them were shown to contribute to IH, mature VSMCs demonstrated a dual function in AVF remodeling, with differentiated VSMCs contributing to medial wall thickening towards venous maturation and dedifferentiated VSMCs contributing to neointimal hyperplasia.[5] The effect of adequate maturation on AVF in NLRP3 deficiency needs to be clarified in future studies.

Collectively, the data presented here suggest that NLRP3 expressed by VSMCs is crucial to the development and progression of AVF failure, which largely depends on the

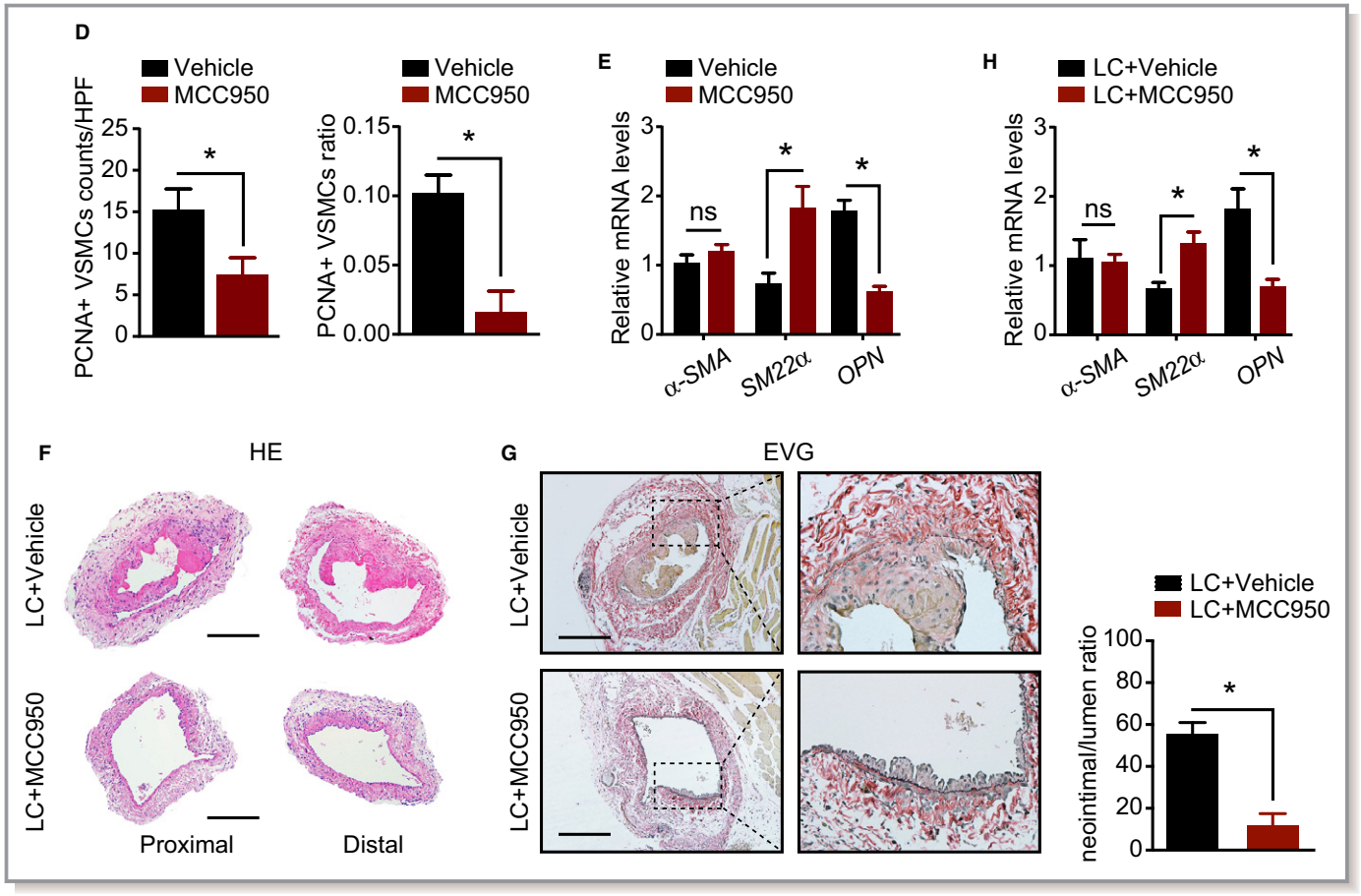


**Figure 7.** Continued.

regulation of Smad2/3 phosphorylation. These findings suggest that specifically targeting VSMCs NLRP3 may be a promising approach for treating AVF failure.

## Acknowledgments

We are thankful to Dr Yuan Sun and Dr Yuanyuan Zhao for their assistance during the study.

## Author Contributions

S. Wang and J. Xia designed the research. X. Ding, J. Chen, C. Wu, G. Wang, C. Zhou, S. Chen, K. Wang, A. Zhang, P. Ye, J. Wu, S. Chen, H. Zhang, and K. Xu did the experiments of the research. X. Ding, J. Chen, and C. Wu collected the data. X. Ding, J. Chen, C. Wu, S. Wang, and J. Xia analyzed the data. X. Ding, J. Chen, and C. Wu wrote the article.

## Sources of Funding

This study was partly supported by grants from the National Natural Science Foundation of China (81730015, 81571560, 81671578, 81570325, and 81500182) and the Nature Science Foundation of Hubei Province (2017CFB357).

## Disclosures

None.

## References

1. Al-Jaishi AA, Oliver MJ, Thomas SM, Lok CE, Zhang JC, Garg AX, Kosa SD, Quinn RR, Moist LM. Patency rates of the arteriovenous fistula for hemodialysis: a systematic review and meta-analysis. *Am J Kidney Dis*. 2014;63:464–478.
2. Dember LM, Beck GJ, Allon M, Delmez JA, Dixon BS, Greenberg A, Himmelfarb J, Vazquez MA, Gassman JJ, Greene T. Effect of clopidogrel on early failure of arteriovenous fistulas for hemodialysis: a randomized controlled trial. *JAMA*. 2008;299:2164–2171.
3. Brahmbhatt A, Remuzzi A, Franzoni M, Misra S. The molecular mechanisms of hemodialysis vascular access failure. *Kidney Int*. 2016;89:303–316.
4. Rothuizen TC, Wong C, Quax PH, van Zonneveld AJ, Rabelink TJ, Rotmans JI. Arteriovenous access failure: more than just intimal hyperplasia? *Nephrol Dial Transplant*. 2013;28:1085–1092.
5. Zhao J, Jourd'heuil FL, Xue M, Conti D, Lopez-Soler RI, Ginnan R, Asif A, Singer HA, Jourd'heuil D, Long X. Dual function for mature vascular smooth muscle cells during arteriovenous fistula remodeling. *J Am Heart Assoc*. 2017;6:e004891. DOI: 10.1161/JAHA.116.004891.
6. Kokubo T, Ishikawa N, Uchida H, Chasnoff SE, Xie X, Mathew S, Hruska KA, Choi ET. Ckd accelerates development of neointimal hyperplasia in arteriovenous fistulas. *J Am Soc Nephrol*. 2009;20:1236–1245.
7. Roy-Chaudhury P, Arend L, Zhang J, Krishnamoorthy M, Wang Y, Banerjee R, Samaha A, Munda R. Neointimal hyperplasia in early arteriovenous fistula failure. *Am J Kidney Dis*. 2007;50:782–790.
8. Roy-Chaudhury P, Spergel LM, Besarab A, Asif A, Ravani P. Biology of arteriovenous fistula failure. *J Nephrol*. 2007;20:150.
9. Zhou R, Yazdi AS, Menu P, Tschopp J. A role for mitochondria in NLRP3 inflammasome activation. *Nature*. 2011;469:221.

10. Franchi L, Eigenbrod T, Muñoz-Planillo R, Nuñez G. The inflammasome: a caspase-1-activation platform that regulates immune responses and disease pathogenesis. *Nat Immunol*. 2009;10:241.
11. Duewell P, Kono H, Rayner KJ, Sirois CM, Vladimer G, Bauernfeind FG, Abela GS, Franchi L, Nunez G, Schnurr M. NLRP3 inflammasomes are required for atherogenesis and activated by cholesterol crystals. *Nature*. 2010;464:1357.
12. Van Hout GP, Bosch L, Ellenbroek GH, De Haan JJ, Van Solinge WW, Cooper MA, Arslan F, De Jager SC, Robertson AA, Pasterkamp G. The selective NLRP3-inflammasome inhibitor MCC950 reduces infarct size and preserves cardiac function in a pig model of myocardial infarction. *Eur Heart J*. 2016;38:828–836.
13. Vandanmagsar B, Youm Y-H, Ravussin A, Galgani JE, Stadler K, Mynatt RL, Ravussin E, Stephens JM, Dixit VD. The NLRP3 inflammasome instigates obesity-induced inflammation and insulin resistance. *Nat Med*. 2011;17:179.
14. Sun H-J, Ren X-S, Xiong X-Q, Chen Y-Z, Zhao M-X, Wang J-J, Zhou Y-B, Han Y, Chen Q, Li Y-H. NLRP3 inflammasome activation contributes to VSMC phenotypic transformation and proliferation in hypertension. *Cell Death Dis*. 2017;8:e3074.
15. Wu D, Ren P, Zheng Y, Zhang L, Xu G, Xie W, Lloyd EE, Zhang S, Zhang Q, Curci JA. NLRP3 (nucleotide oligomerization domain–like receptor family, pyrin domain containing 3)–caspase-1 inflammasome degrades contractile proteins: implications for aortic biomechanical dysfunction and aneurysm and dissection formation. *Arterioscler Thromb Vasc Biol*. 2017;37:694–706.
16. Wu D, Choi J, Coselli J, Shen Y, LeMaire S. NLRP3 inflammasome activates matrix metalloproteinase-9: potential role in smooth muscle cell dysfunction in thoracic aortic disease. *J Surg Res*. 2013;179:204.
17. Bracey NA, Gershkovich B, Chun J, Vilaysane A, Meijndert HC, Wright JR, Fedak PW, Beck PL, Muruve DA, Duff HJ. Mitochondrial NLRP3 protein induces reactive oxygen species to promote Smad protein signaling and fibrosis independent from the inflammasome. *J Biol Chem*. 2014;289:19571–19584.
18. Lech M, Lorenz G, Kulkarni OP, Grosser MO, Stigrot N, Darisipudi MN, Günthner R, Wintergerst MW, Anz D, Susanti HE. NLRP3 and ASC suppress lupus-like autoimmunity by driving the immunosuppressive effects of TGF-β receptor signalling. *Ann Rheum Dis*. 2015;74:2224–2235.
19. Tsai S, Hollenbeck ST, Ryer EJ, Edlin R, Yamanouchi D, Kundi R, Wang C, Liu B, Kent KC. TGF-β through Smad3 signaling stimulates vascular smooth muscle cell proliferation and neointimal formation. *Am J Physiol Heart Circ Physiol*. 2009;297:H540–H549.
20. Goumans M-J, Liu Z, Ten Dijke P. TGF-β signaling in vascular biology and dysfunction. *Cell Res*. 2009;19:116.
21. Wang K, Deng P, Sun Y, Ye P, Zhang A, Wu C, Yue Z, Chen Z, Xia J. MicroRNA-155 promotes neointimal hyperplasia through smooth muscle-like cell-derived rantes in arteriovenous fistulas. *J Vasc Surg*. 2018;67:933–944.e933.
22. Yang H-C, Zuo Y, Fogo AB. Models of chronic kidney disease. *Drug Discov Today Dis Models*. 2010;7:13–19.
23. Kang L, Grande JP, Hillestad ML, Croatt AJ, Barry MA, Katusic ZS, Nath KA. A new model of an arteriovenous fistula in chronic kidney disease in the mouse: beneficial effects of upregulated heme oxygenase-1. *Am J Physiol Renal Physiol*. 2015;310:F466–F476.
24. Huang X, Yue Z, Wu J, Chen J, Wang S, Wu J, Ren L, Zhang A, Deng P, Wang K. MicroRNA-21 knockout exacerbates angiotensin II–induced thoracic aortic aneurysm and dissection in mice with abnormal transforming growth factor-β–SMAD3 signaling. *Arterioscler Thromb Vasc Biol*. 2018;38:1086–1101.
25. Wu C, Ding X, Zhou C, Ye P, Sun Y, Wu J, Zhang A, Huang X, Ren L, Wang K. Inhibition of intimal hyperplasia in murine aortic allografts by administration of a small-molecule TLR4 inhibitor TAK-242. *Sci Rep*. 2017;7:15799.
26. Coll RC, Robertson AA, Chae JJ, Higgins SC, Muñoz-Planillo R, Inserra MC, Vetter I, Dungan LS, Monks BG, Stutz A. A small-molecule inhibitor of the NLRP3 inflammasome for the treatment of inflammatory diseases. *Nat Med*. 2015;21:248.
27. van der Heijden T, Kritikou E, Venema W, van Duijn J, van Santbrink PJ, Slütter B, Foks AC, Bot I, Kuiper J. NLRP3 inflammasome inhibition by MCC950 reduces atherosclerotic lesion development in apolipoprotein E-deficient mice. *Arterioscler Thromb Vasc Biol*. 2017;37:1457–1461.
28. Mridha AR, Wree A, Robertson AA, Yeh MM, Johnson CD, Van Rooyen DM, Haczeyni F, Teoh NC-H, Savard C, Ioannou GN. NLRP3 inflammasome blockade reduces liver inflammation and fibrosis in experimental NASH in mice. *J Hepatol*. 2017;66:1037–1046.
29. Van Rooijen N, Sanders A. Liposome mediated depletion of macrophages: mechanism of action, preparation of liposomes and applications. *J Immunol Methods*. 1994;174:83–93.
30. Alpers CE, Imrey PB, Hudkins KL, Wietecha TA, Radeva M, Allon M, Cheung AK, Dember LM, Roy-Chaudhury P, Shiu Y-T. Histopathology of veins obtained at hemodialysis arteriovenous fistula creation surgery. *J Am Soc Nephrol*. 2017;28:3076–3088.
31. Langer S, Kokozidou M, Heiss C, Kranz J, Kessler T, Paulus N, Krüger T, Jacobs MJ, Lente C, Koeppel TA. Chronic kidney disease aggravates arteriovenous fistula damage in rats. *Kidney Int*. 2010;78:1312–1321.
32. Tong X, Hou X, Wason C, Kopel T, Cohen RA, Dember LM. Smooth muscle nitric oxide responsiveness and clinical maturation of hemodialysis arteriovenous fistulae. *Am J Pathol*. 2017;187:2095–2101.
33. Ferrer LM, Monroy AM, Lopez-Pastrana J, Nanayakkara G, Cueto R, Li Y-F, Li X, Wang H, Yang X-F, Choi ET. Caspase-1 plays a critical role in accelerating chronic kidney disease-promoted neointimal hyperplasia in the carotid artery. *J Cardiovasc Transl Res*. 2016;9:135–144.
34. Li P, Li Y-L, Li Z-Y, Wu Y-N, Zhang C-C, Xi A, Wang C-X, Shi H-T, Hui M-Z, Xie B. Cross talk between vascular smooth muscle cells and monocytes through interleukin-1β/interleukin-18 signaling promotes vein graft thickening. *Arterioscler Thromb Vasc Biol*. 2014;34:2001–2011.
35. Bessueille L, Fakhry M, Hamade E, Badran B, Magne D. Glucose stimulates chondrocyte differentiation of vascular smooth muscle cells and calcification: a possible role for IL-1β. *FEBS Lett*. 2015;589:2797–2804.
36. Choi J, Wu D, Zheng Y, Zhang L, Coselli J, Shen Y, LeMaire S. Activation of the NLRP3 inflammasome cascade amplifies TGFB signaling during acute ascending aortic stress. *J Surg Res*. 2014;186:597.
37. Proudfoot D, Dautova Y, Kozlova D, Epple M, Bootman M. Calcification stimulates inflammatory signalling pathways in human vascular smooth muscle cells. *Atherosclerosis*. 2016;244:e9–e10.
38. Tangi TN, Elmabsout AA, Bengtsson T, Sirsjö A, Fransén K. Role of NLRP3 and CARD8 in the regulation of TNF-α induced IL-1β release in vascular smooth muscle cells. *Int J Mol Med*. 2012;30:697.
39. Kim EJ, Park SY, Baek SE, Jang MA, Kim CD. HMGB1 promotes IL-1beta production in vascular smooth muscle cells via activation of NLRP3 inflammasome. *Atherosclerosis*. 2017;263:e113.
40. Wasse H, Huang R, Naqvi N, Smith E, Wang D, Husain A. Inflammation, oxidation and venous neointimal hyperplasia precede vascular injury from AVF creation in CKD patients. *J Vasc Access*. 2012;13:168–174.
41. Weiss MF, Scivittaro V, Anderson JM. Oxidative stress and increased expression of growth factors in lesions of failed hemodialysis access. *Am J Kidney Dis*. 2001;37:970–980.
42. Hu H, Patel S, Hanisch JJ, Santana JM, Hashimoto T, Bai H, Kudze T, Foster TR, Guo J, Yatsula B. Future research directions to improve fistula maturation and reduce access failure. *Semin Vasc Surg*. 2016;29:153–171.

# SUPPLEMENTAL MATERIAL

**Table S1. Clinical Characteristics of the Study Subjects.**

| Characteristic | Occluded AVFs (n=6) | Control (n=5) | *P*-value |
|---|---|---|---|
| Type of vein | Cephalic vein | Great saphenous vein* | - |
| Female sex | 3 (50%) | 2 (40%) | - |
| Age, years | 53.5±8.849 | 55.4±8.355 | 0.7246 |
| Body mass index, $kg/m^2$ | 29.38±5.768 | 29.00±5.431 | 0.9128 |
| Presence of diabetes | 4 (66.7%) | 3 (60%) | - |
| Presence of hypertension | 6 (100%) | 5 (100%) | - |
| Presence of peripheral vascular disease† | 1 (16.7%) | 0 (0%) | - |
| Presence of uraemia | 6 (100%) | 0 (0%) | - |

Data are expressed as mean±standard deviation; data were analysed by unpaired *t* test.

*The healthy cephalic vein may serve as a better control, practically and ethically, we can only use the excess healthy saphenous vein as a control from patients undergoing coronary artery bypass surgery.

†This included a history of claudication, lower extremity angioplasty or bypass surgery, nontraumatic amputation, or varicose veins.

**Table S2. qPCR primers used for mRNA expression analysis.**

| *Gene* | Forward | Reverse |
|---|---|---|
| *NLRP3* | TGCTCTTCACTGCTATCAAGCCCT | ACAAGCCTTTGCTCCAGACCCTAT |
| *α-SMA* | GTGACATCGACATCAGGAAAGA | GATCCACATCTGCTGGAAGG |
| *SM22α* | TGAAGGCGGCTGAGGACTAT | TCTGTTGCTGCCCATCTGAA |
| *OPN* | CTTTCACTCCAATCGTCCCTA | GCTCTCTTTGGAATGCTCAAGT |
| *IL-1α* | ACTGCCCAAGATGAAGACCA | CCGTGAGTTTCCCAGAAGAA |
| *IL-1β* | CAACCAACAAGTGATATTCTCCATG | GATCCACACTCTCCAGCTGCA |
| *IL-6* | CTGCAAGAGACTTCCATCCAGTT | GAAGTAGGGAAGGCCGTGG |
| *Tnf-α* | TCTTCTGTCTACTGAACTTCG | GAAGATGATCTGAGTGTGAGG |
| *Ccl2* | TTTTGTCACCAAGCTCAAGAGA | ATTAAGGCATCACAGTCCGAGT |
| *Cxcl12* | CATCCATCCATCCATCCA | TTCAGGGTCATGGAGACAGT |
| *Cx3cl1* | GTTCTTCCATTTGTGTA | CTGTGTCGTCTCCAGGACAA |
| *PCNA* | TTGCACGTATATGCCGAGACC | GGTGAACAGGCTCATTCATCTCT |
| *Gapdh* | GAACCCTAAGGCCAACCGTGAAAGAT | ACCGCTCGTTGCCAATAGTGATG |

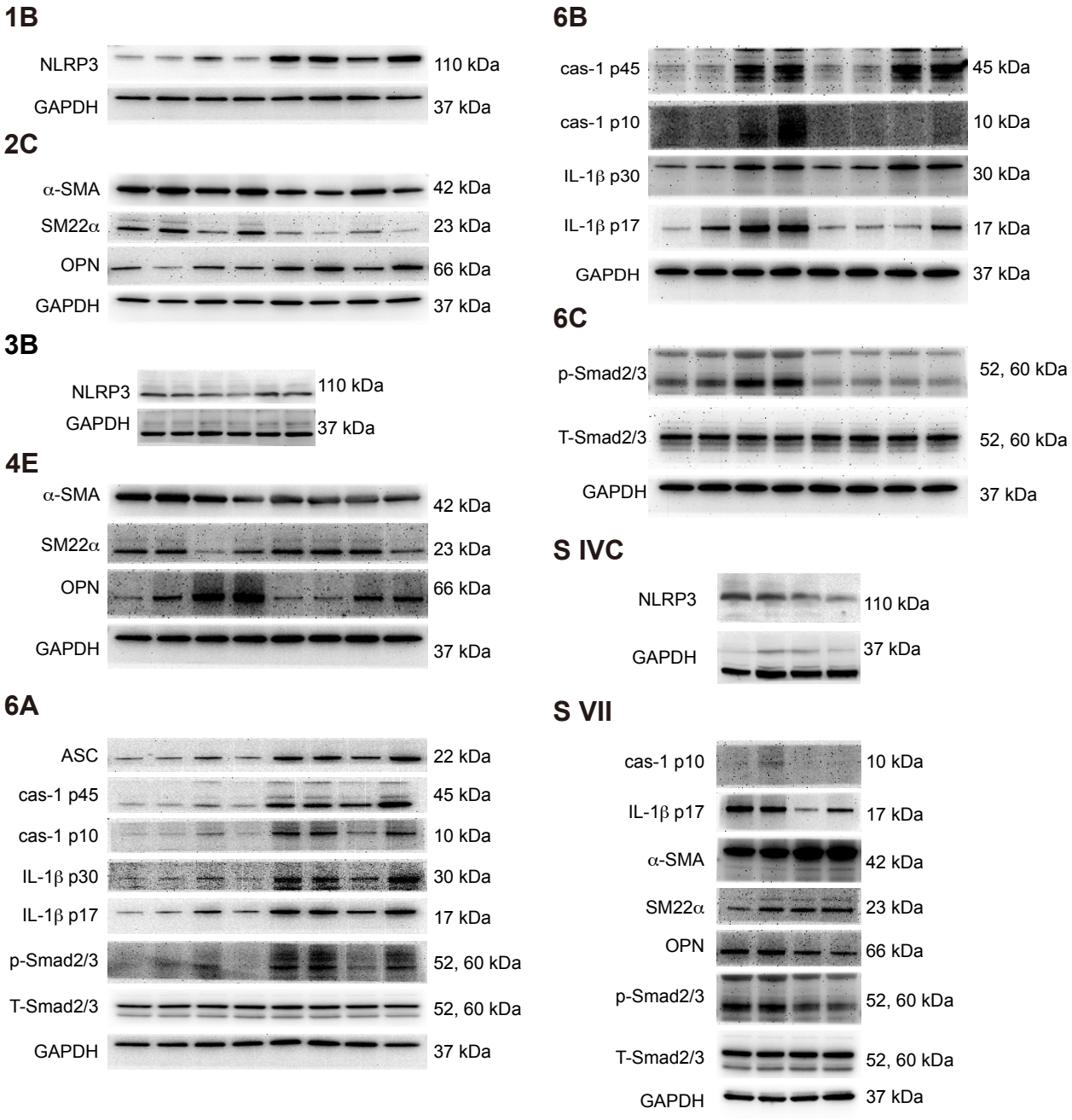


**Figure S1. Image of the original uncropped blots of a representative Western blot.**

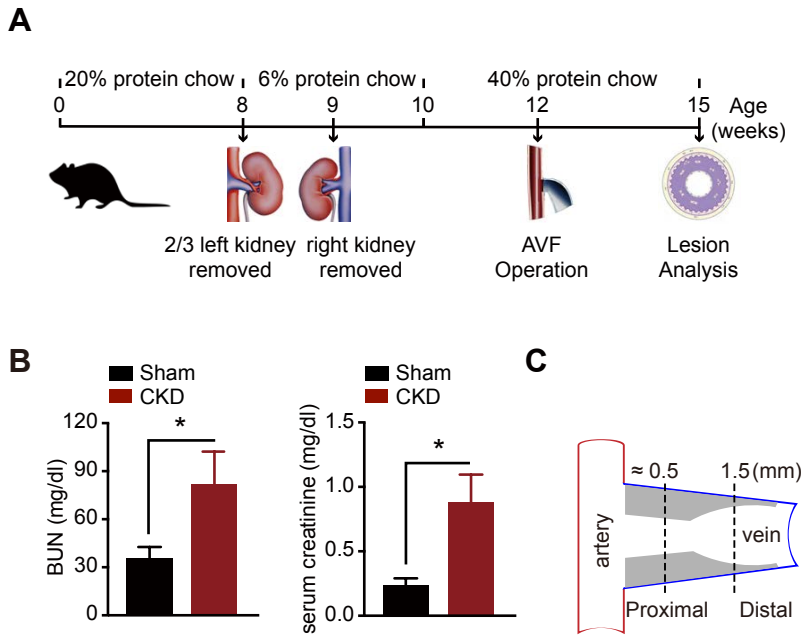


**Figure S2. A**, The experimental design used to establish CKD and AVFs in mice. **B**, The serum of mice was collected 3 weeks after right kidney removal, BUN (**left**) and serum creatinine (**right**) levels were assessed. **C**, The distal and proximal regions in the outflow veins of AVFs were selected for further studies. **P*<0.05; ns: not statistically significant; data were analysed by the unpaired *t* test. CKD, chronic kidney disease; AVF, arteriovenous fistula; BUN, blood urea nitrogen.

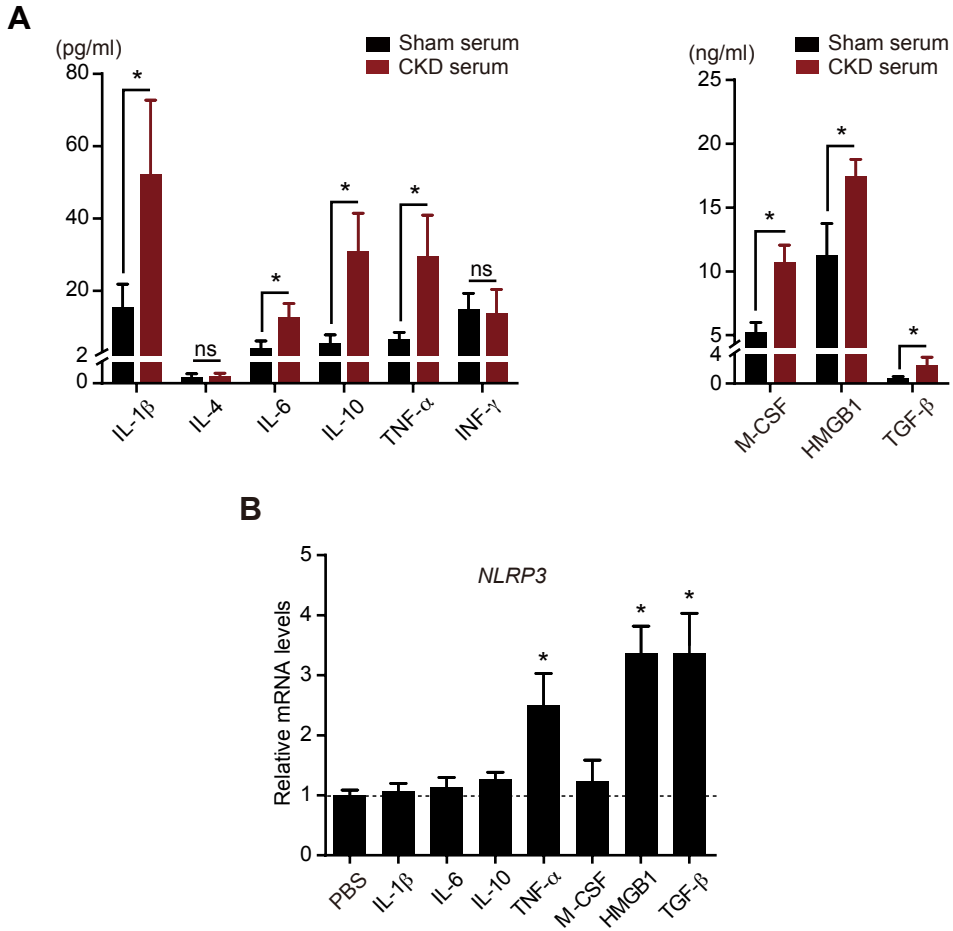


**Figure S3. A**, Serum from CKD or sham mice were analysed using the ELISA. **B**, *NLRP3* mRNA expression in WT VSMCs was measured by qPCR (VSMCs were harvested after 24 hours of starvation and 24 hours of normal medium cultured in the presence of IL-1β (1ng/ml), IL-6 (1ng/ml), IL-10 (1ng/ml), TNF-α (1ng/ml), M-CSF (10ng/ml), HMGB1 (10ng/ml) and TGF-β (10ng/ml) stimulation; PBS was used as a control). **P*<0.05; ns: not statistically significant; data were analysed by the unpaired *t* test. ELISA, enzyme-linked immunosor-bent assay; CKD, chronic kidney disease; NLRP3, nucleotide-binding oligomerisation domain-like receptor protein 3; mRNA, messenger RNA; WT, wild-type; VSMC, vascular smooth muscle cell; qPCR, quantitative real-time polymerase chain reaction; IL, interleukin; TNF, tumour necrosis factor; M-CSF, macrophage colony-stimulating factor; HMGB1, high-mobility group protein 1; TGF, transforming growth factor; PBS, phosphate-buffered saline.

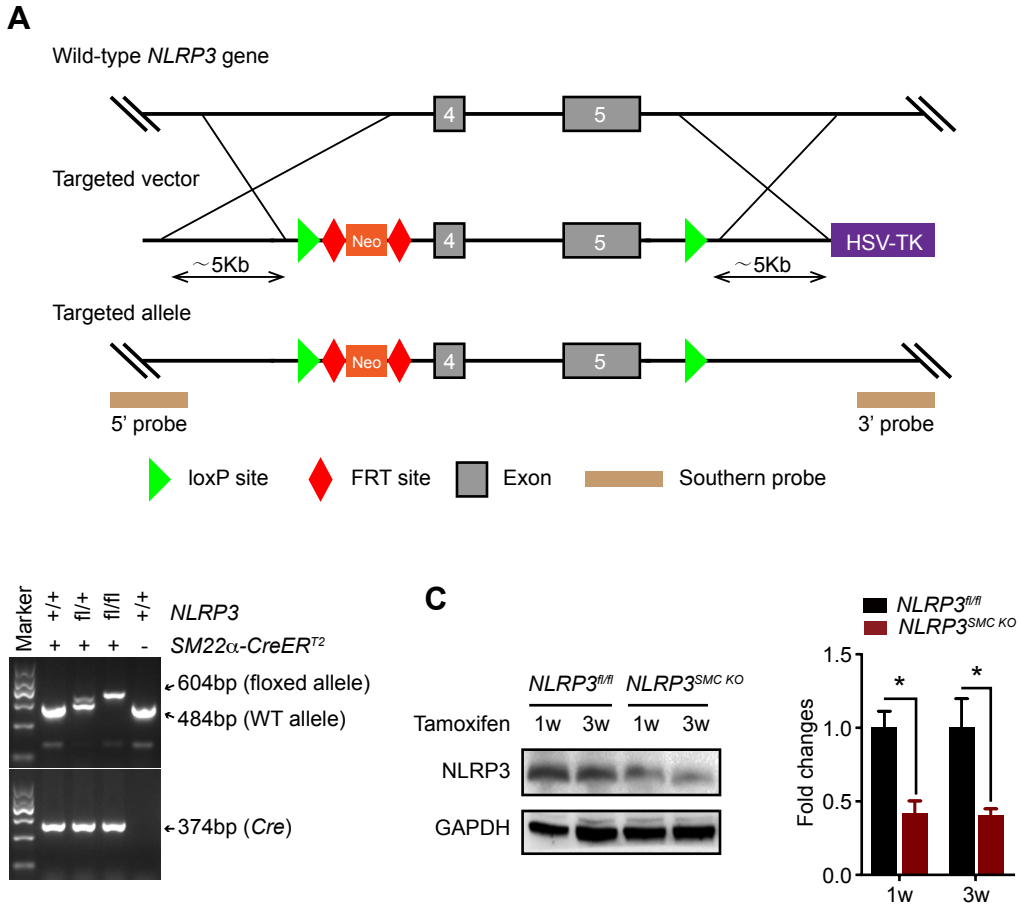


**Figure S4. A**, Schematic illustration of *NLRP3*$^{fl/fl}$ mice generation. **B**, Mice genotyping was confirmed by polymerase chain reaction. **C**, Western blot results for NLRP3 expression levels in artery tissue from *NLRP3*$^{fl/fl}$ and *NLRP3*$^{SMC\ KO}$ mice 1 week or 3 weeks after tamoxifen treatment. Quantification is shown in the **right**. **P*<0.05; ns: not statistically significant; data were analysed by the unpaired *t* test. NLRP3, nucleotide-binding oligomerisation domain-like receptor protein 3; *NLRP3*$^{SMC\ KO}$, smooth-muscle-specific knockout nucleotide-bind-ing oligomerisation domain-like receptor protein 3.

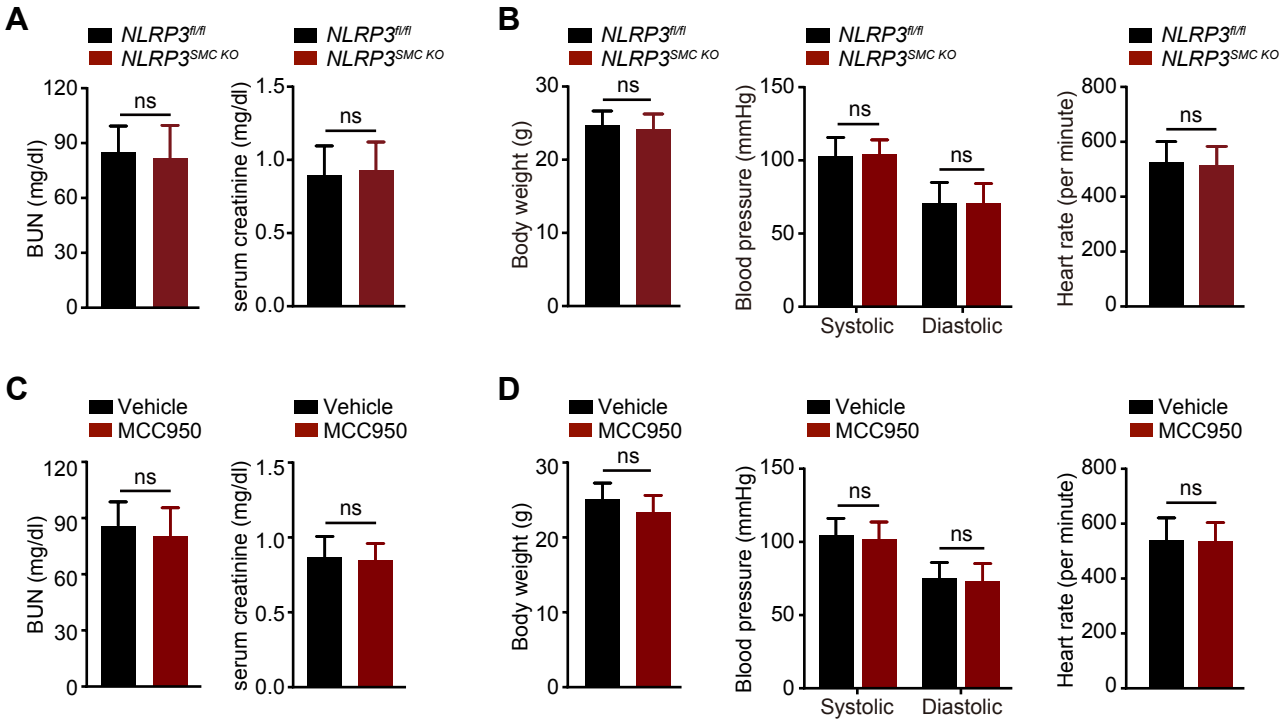


**Figure S5. A**, Values of BUN (**left**) and serum creatinine (**right**) of *NLRP3*$^{fl/fl}$ and *NLRP3*$^{SMC\ KO}$ mice on POD 21. **B**, Body weight (**left**), blood pressure (**middle**), and heart rate (**right**) of *NLRP3*$^{fl/fl}$ and *NLRP3*$^{SMC\ KO}$ mice on POD 21. **C**, Values of BUN (**left**) and serum creatinine (**right**) of WT mice on POD 21 in the presence of MCC950 or vehicle. **D**, Body weight (**left**), blood pressure (**middle**), and heart rate (**right**) of WT mice on POD 21 in the presence of MCC950 or vehicle. **P*<0.05; ns: not statistically significant; data were analysed by the unpaired *t* test. BUN, blood urea nitrogen; NLRP3, nucleotide-binding oligomerisation domain-like receptor protein 3; *NLRP3*$^{SMC\ KO}$, smooth-muscle-specific knockout nucleotide-binding oligomerisation domain-like receptor protein 3; POD, postoperative days; WT, wild-type.

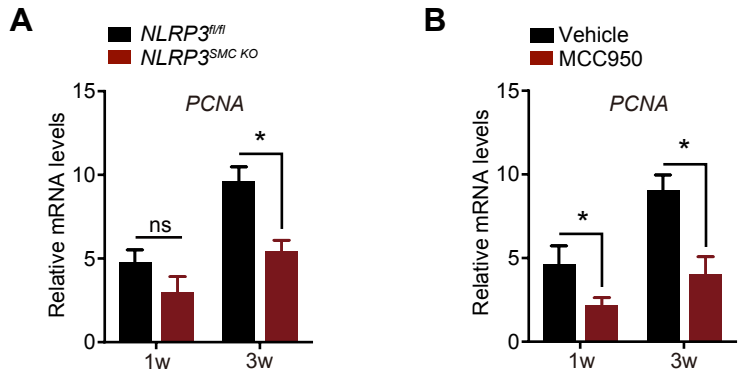


**Figure S6. A**, *PCNA* mRNA expression was measured by qPCR in the outflow veins of the AVFs from CKD *NLRP3*$^{fl/fl}$ and CKD *NLRP3*$^{SMC\ KO}$ mice 1 week or 3 weeks after AVF construction; the contralateral jugular vein was used as a control. **B**, *PCNA* mRNA expression was measured by qPCR in the outflow veins of the AVFs from vehicle-treated and MCC950-treated CKD WT mice 1 week or 3 weeks after AVF construction; the contralateral jugular vein was used as a control. *$P$<0.05; ns: not statistically significant; data were analysed by the unpaired *t* test. PCNA, proliferating cell nuclear antigen; mRNA, messenger RNA; qPCR, quantitative real-time polymerase chain reaction; AVF, arteriovenous fistula; CKD, chronic kidney disease; NLRP3, nucleotide-binding oligomerisation domain-like receptor protein 3; *NLRP3*$^{SMC\ KO}$, smooth-muscle-specific knockout nucleotide-binding oligomerisation domain-like receptor protein 3; WT, wild-type.

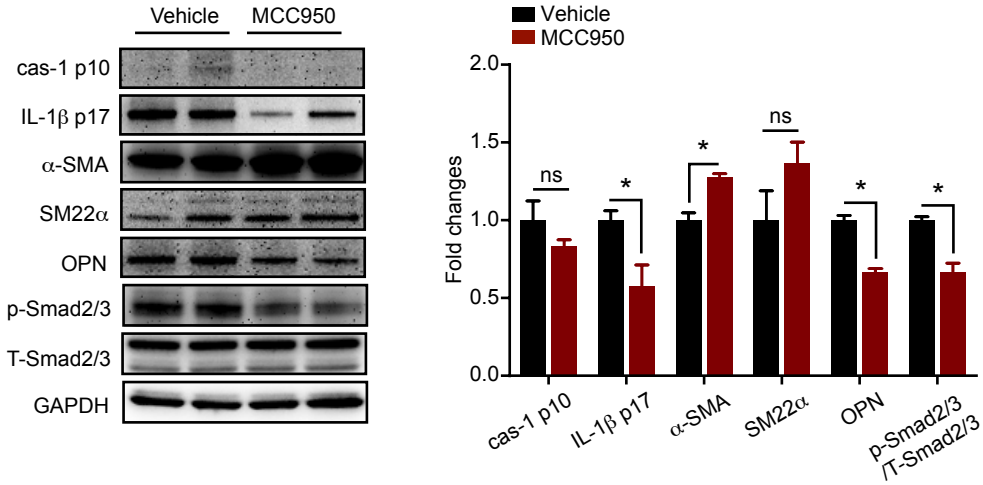


**Figure S7.** Caspase-1 p10, IL-1β p17, α-SMA, SM22α, OPN, Smad2/3 protein levels in WT VSMCs were determined using Western blot analysis (VSMCs were harvested after 24 hours' starvation and 48 hours' 20% CKD serum stimulation in the presence of a vehicle or 50 μM MCC950). Quantification is shown in the **right**. **P*<0.05; ns: not statistically significant; data were analysed by the unpaired *t* test. IL, interleukin; α-SMA, alpha-smooth muscle actin; SM22α, smooth muscle protein 22 alpha; OPN, osteopontin; WT, wild-type; VSMC, vascular smooth muscle cell; CKD, chronic kidney disease.

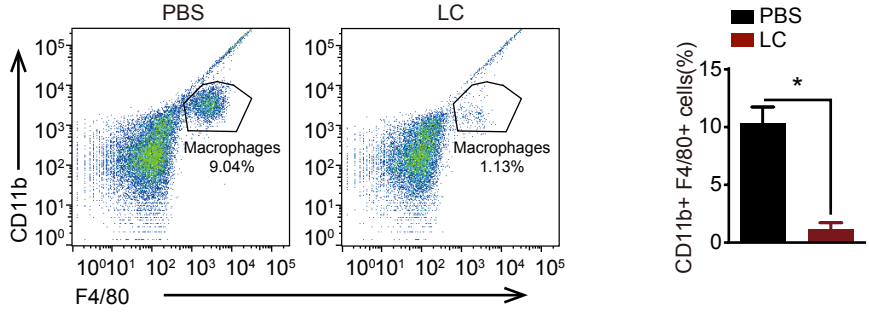


**Figure S8.** Results of flow cytometry analysis of the peripheral blood from WT mice 1 week after LC or PBS liposome treatment. Quantification is shown in the **right**. **P*<0.05; ns: not statistically significant; data were analysed by the unpaired *t* test. WT, wild-type; LC, clodronate liposomes; PBS, phosphate-buffered saline.